General Disclaimer

One or more of the Following Statements may affect this Document

- This document has been reproduced from the best copy furnished by the organizational source. It is being released in the interest of making available as much information as possible.

- This document may contain data, which exceeds the sheet parameters. It was furnished in this condition by the organizational source and is the best copy available.

- This document may contain tone-on-tone or color graphs, charts and/or pictures, which have been reproduced in black and white.

- This document is paginated as submitted by the original source.

- Portions of this document are not fully legible due to the historical nature of some of the material. However, it is the best reproduction available from the original submission.

Produced by the NASA Center for Aerospace Information (CASI)

5.0 Copies

NATIONAL AERONAUTICS AND SPACE ADMINISTRATION

Technical Report 32-1242

Summary of a Study of the Low-Pressure Combustion of Solid Propellants

L. D. Strand

N68-21865

FACILITY FORM 602

(ACCESSION NUMBER) (THRU)

34 (PAGES) 1 (CODE)

CR-94238 (NASA CR OR TMX OR AD NUMBER) 27 (CATEGORY)

CFSTI PRICE(S) $

Hard copy (HC) 3.00

Microfiche (MF) .65

ff 653 July 65

JET PROPULSION LABORATORY

CALIFORNIA INSTITUTE OF TECHNOLOGY

PASADENA, CALIFORNIA

April 15, 1968

NATIONAL AERONAUTICS AND SPACE ADMINISTRATION

Technical Report 32-1242

Summary of a Study of the Low-Pressure Combustion of Solid Propellants

L. D. Strand

Approved by:

Winston Gin, *Manager*
Solid Propellant Engineering Section

JET PROPULSION LABORATORY
CALIFORNIA INSTITUTE OF TECHNOLOGY
PASADENA, CALIFORNIA

April 15, 1968

Acknowledgment

The author expresses his appreciation to Anthony Rasmussen, who performed the test firings, and to Donald Maxeiner and Robert Hanson for the motion picture photography.

PRECEDING PAGE BLANK NOT FILMED.

Contents

Table

PRECEDING PAGE BLANK NOT FILMED.

Contents (contd)

Figures

Contents (contd)

Figures (contd)

Abstract

The phenomena of solid propellant low-pressure instability and extinguishment were investigated. The investigation included a motor firing test program, a series of transparent motor tests, rather extensive reduction and analyses of the test data, and attempts to develop theoretical models that would accurately describe the experimental phenomena. Under the motor firing program, information on the influence of the following propellant variables on low-pressure extinction was obtained: (1) propellant configuration, (2) aluminum/oxidizer concentration ratio, (3) aluminum particle size, (4) oxidizer particle size, and (5) binder type. The series of transparent motor tests which were conducted were designed to gain insight into the actual mechanisms causing low-pressure extinction. Further reduction and analysis of the motor firing test data yielded information on the point of onset of instability, the frequency dependence of the instability on the rocket chamber pressure and L^*, and the significance of the pressure oscillation rate-of-depressurization on the extinction process. Comparison of the low-pressure combustion data with existing theoretical models resulted in qualitative agreement only. Low-pressure L^* extinction is concluded to be due to self-induced pressure perturbations and is believed to be a manifestation of the same phenomenon controlling rapid depressurization combustion extinction.

Summary of a Study of the Low-Pressure Combustion of Solid Propellants

I. Introduction

During the course of development of a high-performance motor at JPL, an attempt was made to markedly decrease the operating chamber pressure (Ref. 1). On attempting to ignite the motor, ignition occurred, but the motor extinguished itself shortly after ignition. A second attempt using a different nozzle with a slightly smaller throat area resulted in the same phenomenon, but the motor continued to ignite and extinguish repeatedly (chuff) until finally stabilizing and burning normally to propellant exhaustion. This experience led to further tests in this low pressure region, the results of which revealed an apparent correlation between the minimum stable pressure region and the motor port-to-throat area ratio. Additional test firings with regressive burning propellant configurations showed that the motors could extinguish without the presence of an ignition transient and suggested the existence of a threshold pressure below which stable combustion could not be sustained in a rocket system.

Abnormal solid propellant combustion under low-pressure conditions was not a new phenomenon. The chuffing phenomenon and the conditions under which it occurred had been described in 1944 in Ref. 2.

An investigation of this low-pressure combustion phenomenon was begun and has continued for the past several years. This report will attempt to summarize the work and the results obtained under the program and give the resulting conclusions that have been drawn as to the mechanisms controlling this phenomenon.

II. Motor Firing Test Program

A. Test Description

Low-pressure instability and extinguishment data for a number of composite solid propellants were acquired using threaded, and later, flanged versions of a small 3-in. ID test motor and several types of regressive burning propellant charges. The flanged motor version is shown in Figs. 1 and 2. The motor L^*[1] and chamber pressure P_c were varied by changing both the motor

[1]Motor free volume/throat-area ratio.

chamber length, from 4½ to 12½ in., and the nozzle throat diam. Composite propellant variables included (1) the propellant configuration, (2) aluminum/oxidizer concentration ratio, (3) aluminum particle size, (4) ammonium perchlorate oxidizer particle size, and (5) binder type.[2] Polyurethane was the standard binder used, and ammonium perchlorate was the oxidizer in all cases.

Details of the test apparatus, instrumentation, and procedure have been covered in detail in Ref. 3 and will not be repeated here. The propellant charges were ignited in the stable operating pressure region, burned regressively with decreasing pressure into the unstable pressure region, and ultimately ceased burning (extinguished). For a majority of the test data records, low-frequency, low-amplitude oscillations in pressure appeared to occur prior to extinction of combustion, Fig. 3. These oscillations decreased in frequency and grew in amplitude as the pressure in the motor chambers lowered. In all cases the oscillations occurred at frequencies well below the characteristic acoustic frequencies of the motor chambers. The motors were exhausted into an evacuated tank, thereby preventing reignition of the propellant charges following extinction and allowing the propellant dimensions at extinction to be measured. In earlier regressive burning test firings at atmospheric conditions, the propellant had invariably begun to chuff following extinction and continued to do so until all of the propellant was consumed.

The information that was originally obtained from the test data records consisted of the mean chamber pressure, motor L^*, and frequency of pressure oscillations, where measurable, at combustion extinction. This material has been published in earlier reports and will just be summarized briefly here.

[2]Very little testing with the latter two.

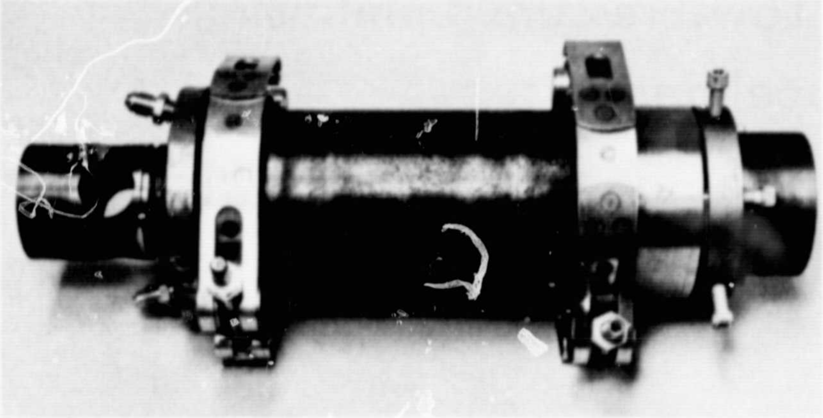

Fig. 1. Test motor, 3-in. ID, assembled

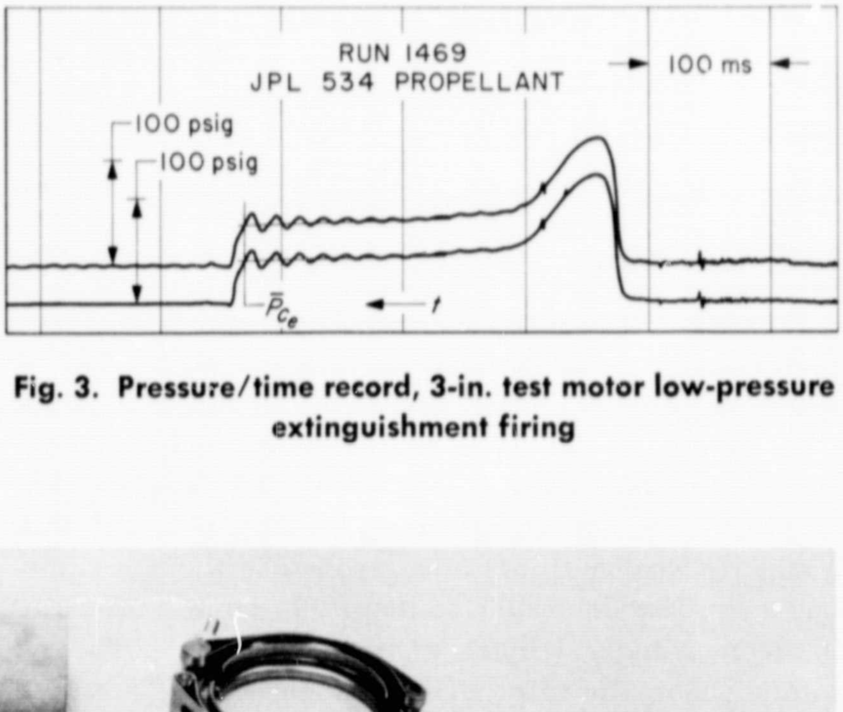

Fig. 3. Pressure/time record, 3-in. test motor low-pressure extinguishment firing

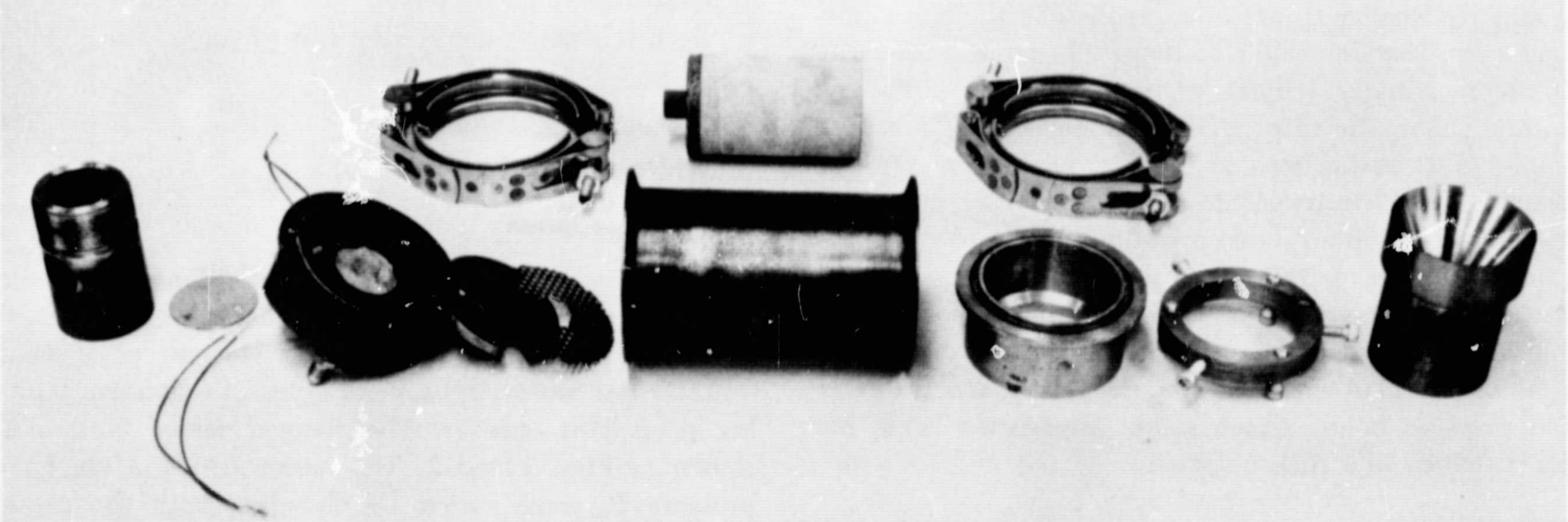

Fig. 2. Test motor, 3-in. ID, disassembled

B. Propellant Variables Investigated and Extinction Results

1. Propellant configuration. Two sets of experiments were reported in Refs. 3 and 4. The first consisted of approximately 40 firings using JPL 534 propellant (2% aluminum, 1.5% copper chromite). Burning rate data for the propellant is shown in Fig. 4. The primary purpose of these tests was to determine the effects, if any, of the propellant grain geometry on the low-pressure extinction. The geometries used consisted of (1) cylinder, (2) cone, (3) regressive end burner, and (4) a regressive tubular. On the basis of the theoretical instability model reported in Ref. 5 the motor L^* values and mean chamber pressures measured at extinction $\overline{P}_{c_e}$ were plotted on log-log coordinates (Fig. 5).[3] The correlation over this extinction pressure range of from 16–64 psia was excellent. The possible theoretical aspects of this L^* correlation will be discussed later. As is evident from Fig. 5, there seemed to be no effect of the propellant geometry on the L^*-pressure extinction correlation. The frequency of pressure oscillations immediately prior to extinction was calculated, where measurable, and correlated both with L^* and $\overline{P}_{c_e}$ (Figs. 6 and 7).

[3]The limiting pressure for combustion, as determined in a slowly vented Crawford bomb, was measured to be 6 psia.

2. Aluminum/oxidizer concentration ratio. The second series of experiments were conducted to determine the effect of the magnitude of a propellant's aluminum concentration on the L^* correlation and determine if the correlation would be valid for a different propellant. The tests were conducted using the second, third, and fourth propellants listed in Table 1, JPL 540 and two modified formulations. The Mod A and Mod B formulations were obtained by replacing all and one-half, respectively, of the aluminum in the standard JPL 540 propellant with oxidizer; this resulted in a decreased aluminum/oxidizer concentration ratio. The burning rate data for the three propellants, shown in Fig. 8, was obtained by using the Crawford bomb strand burner. At low pressures ($\leq$ 50 psia) the replacement of aluminum with oxidizer raised the burning rate, but had little effect on the burning rate pressure exponent, n.

The L^*-extinction-pressure relationships for the three propellants were established by 3-in. diam motor firings. For these and all subsequent tests only cylindrical externally burning propellant charges, 2½-in. in diam × 4–4½ in. long, inhibited on the head end, were used (Fig. 9). The extinguished grains had a smoother appearance than the pre-test machined surface. Fine granular material, probably quenched aluminum agglomerates, often remained on the surface. The test data obtained

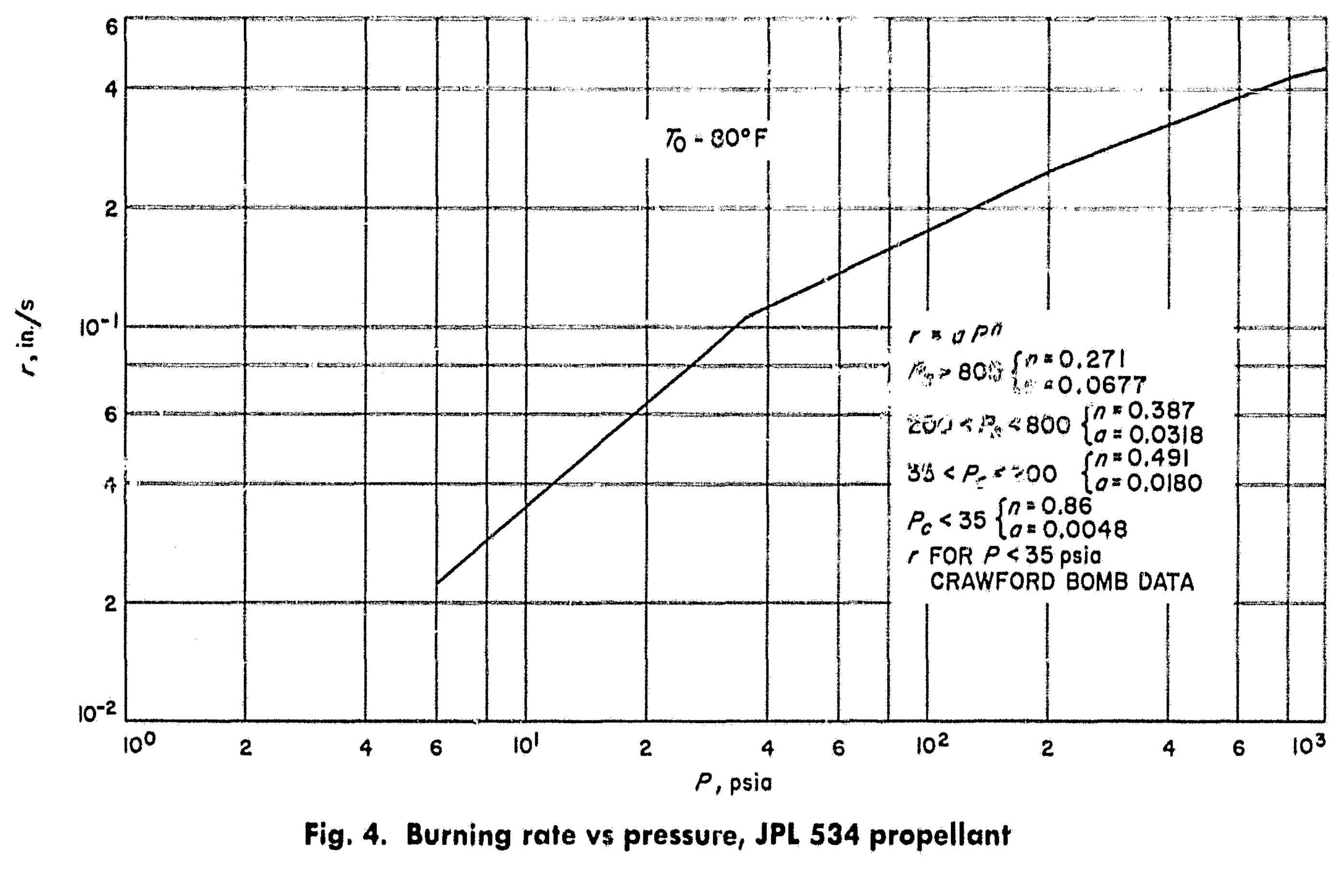

Fig. 4. Burning rate vs pressure, JPL 534 propellant

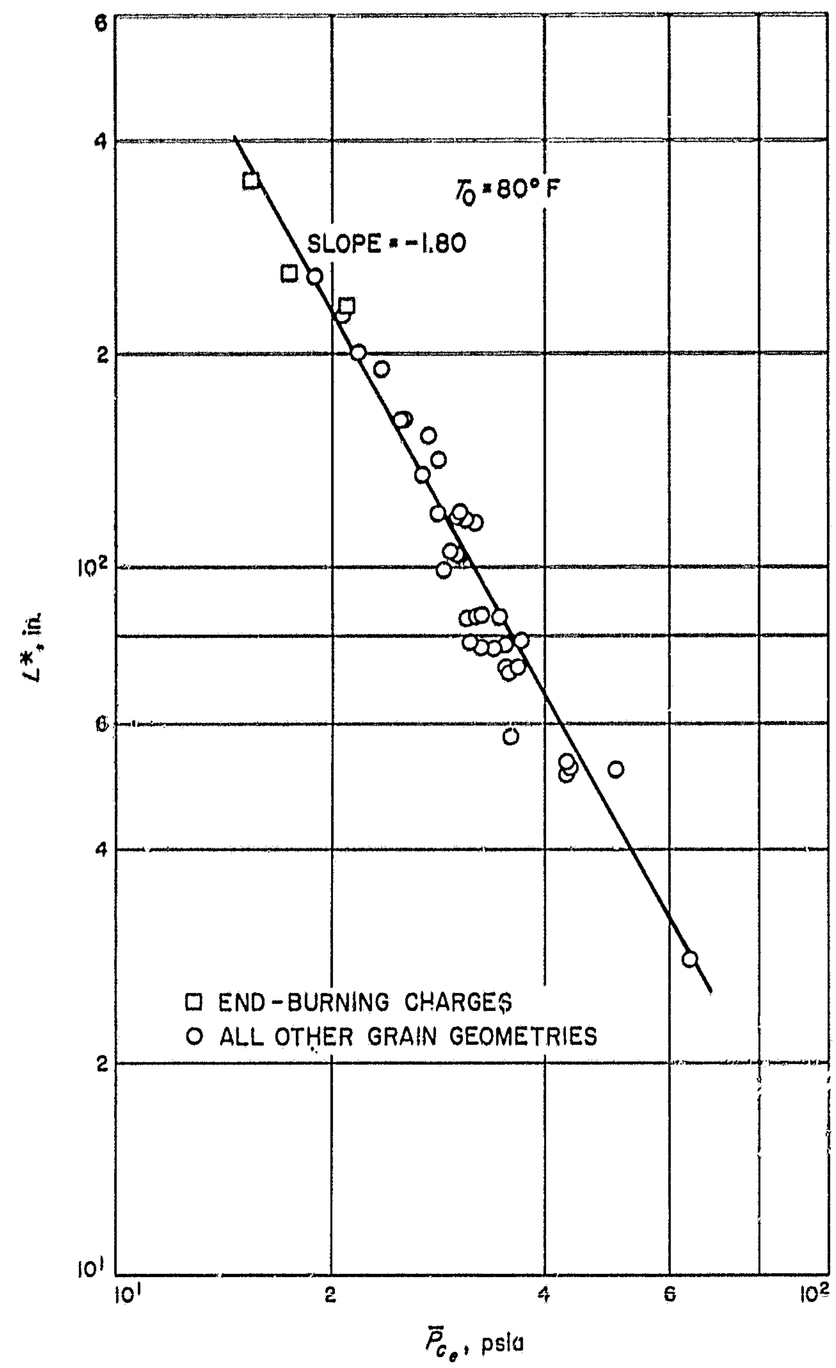

Fig. 5. *L vs mean chamber pressure at combustion extinction, JPL 534 propellant**

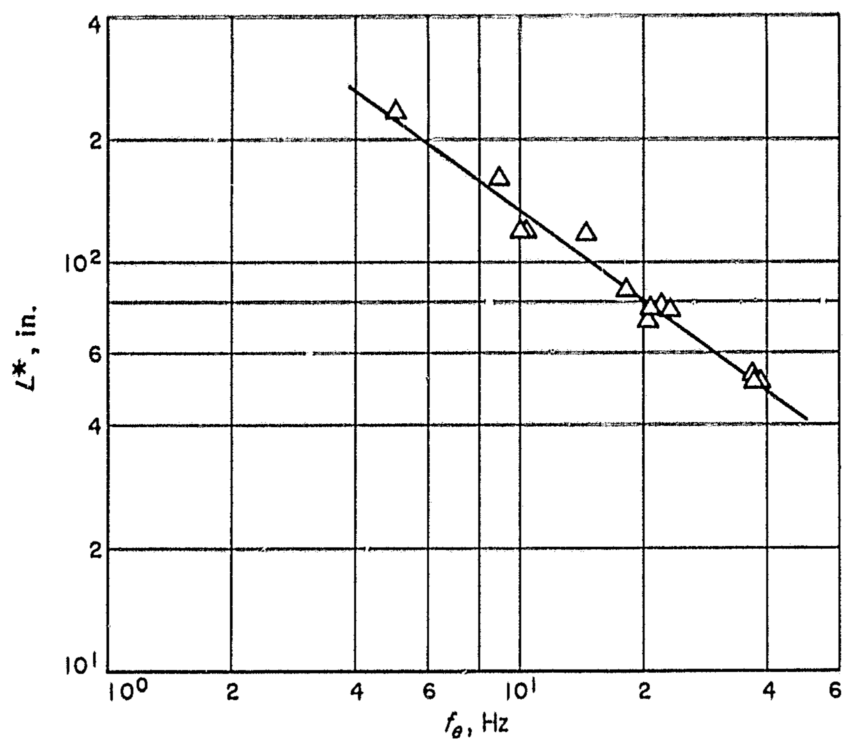

Fig. 6. *L vs pressure oscillation frequency at combustion extinction, JPL 534 propellant**

Table 1. Experimental propellants

Propellant designation	Oxidizer, fine grind mass median diam = 17 μm		Aluminum, %	Aluminum mass median diam, μm	Aluminum/oxidizer concentration ratio
	Coarse/fine distribution	Coarse grind mass median diam, μm			
JPL 534	70/30, BIMODAL	170	2	7	Decreased
JPL 540			16	7	Standard
JPL 540 Mod A			0	—	Zero
JPL 540 Mod B			8	7	Decreased
JPL 540 Mod 1			16	31	Standard
JPL 540 Mod 2		↓		15–17	
JPL 540 Mod 3	↓	400		31	
JPL 540 Mod 4	100/0, UNIMODAL	400	↓	7	↓

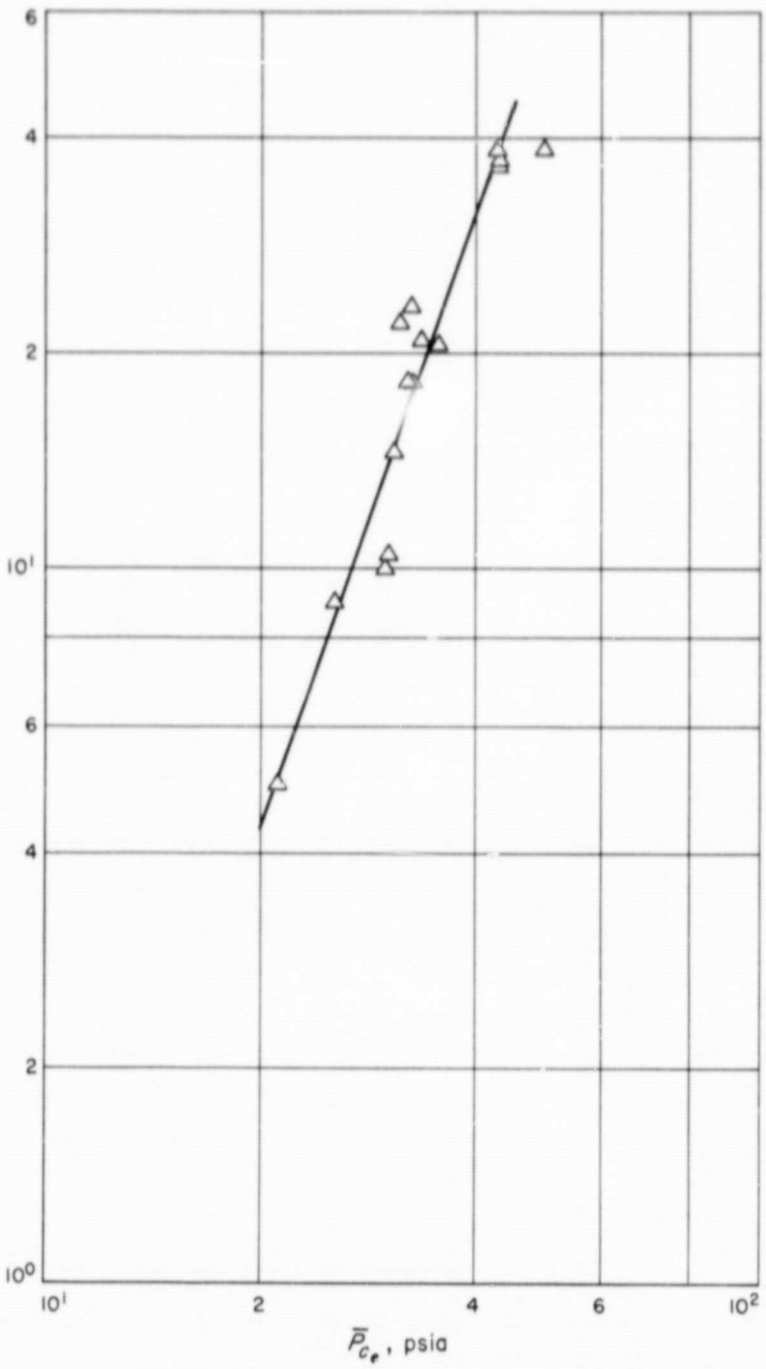

Fig. 7. Pressure oscillation frequency vs mean chamber pressure at combustion extinction, JPL 534 propellant

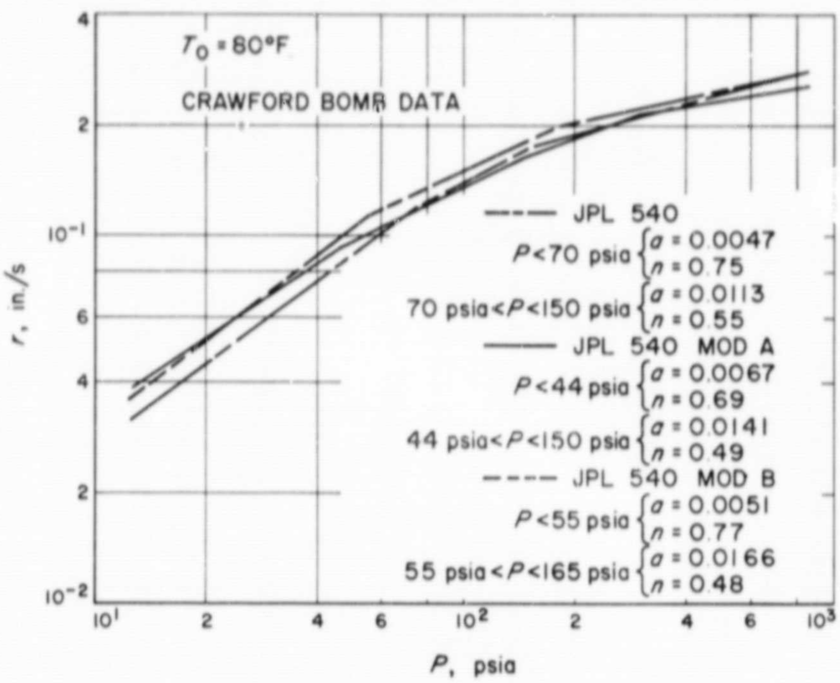

Fig. 8. Burning rate vs pressure, JPL 540, Mod A, and Mod B propellants

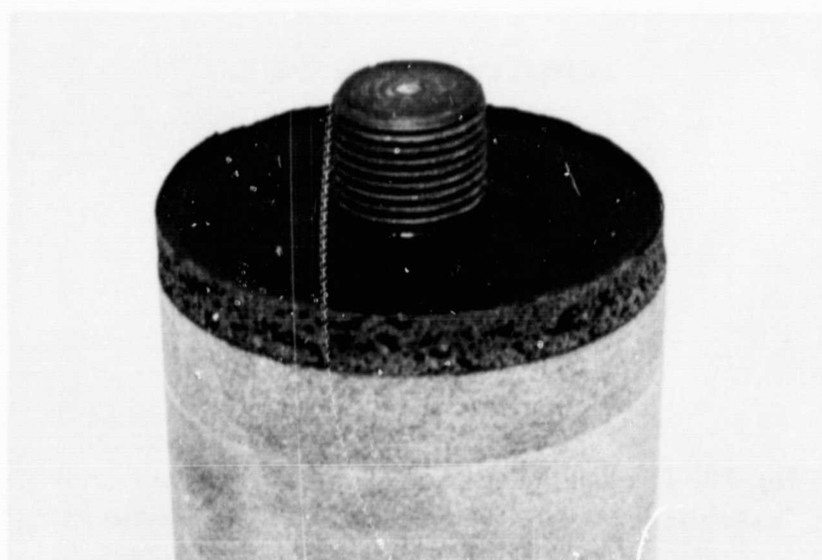

Fig. 9. Propellant charge, 2½ × 4 in.

are plotted in Fig. 10. The log-log plots of L^* vs $\overline{P}_{c_e}$ for the three propellants had an increasing negative slope (-1.77 to -5.85) and moved into a higher pressure region with increasing aluminum/oxidizer concentration ratio, markedly reducing the pressure sensitivity of the L^* correlation.

The frequency of pressure oscillations immediately prior to combustion extinction correlated with the mean chamber pressure (Fig. 11) and motor L^* (Fig. 12) at extinction. Increasing the aluminum/oxidizer concentration ratio resulted in a decrease in the frequency of oscillations at extinction.

3. ***Aluminum particle size.*** The effect of the coarseness of the aluminum additive on the low-pressure unstable combustion characteristic was studied using the fifth and

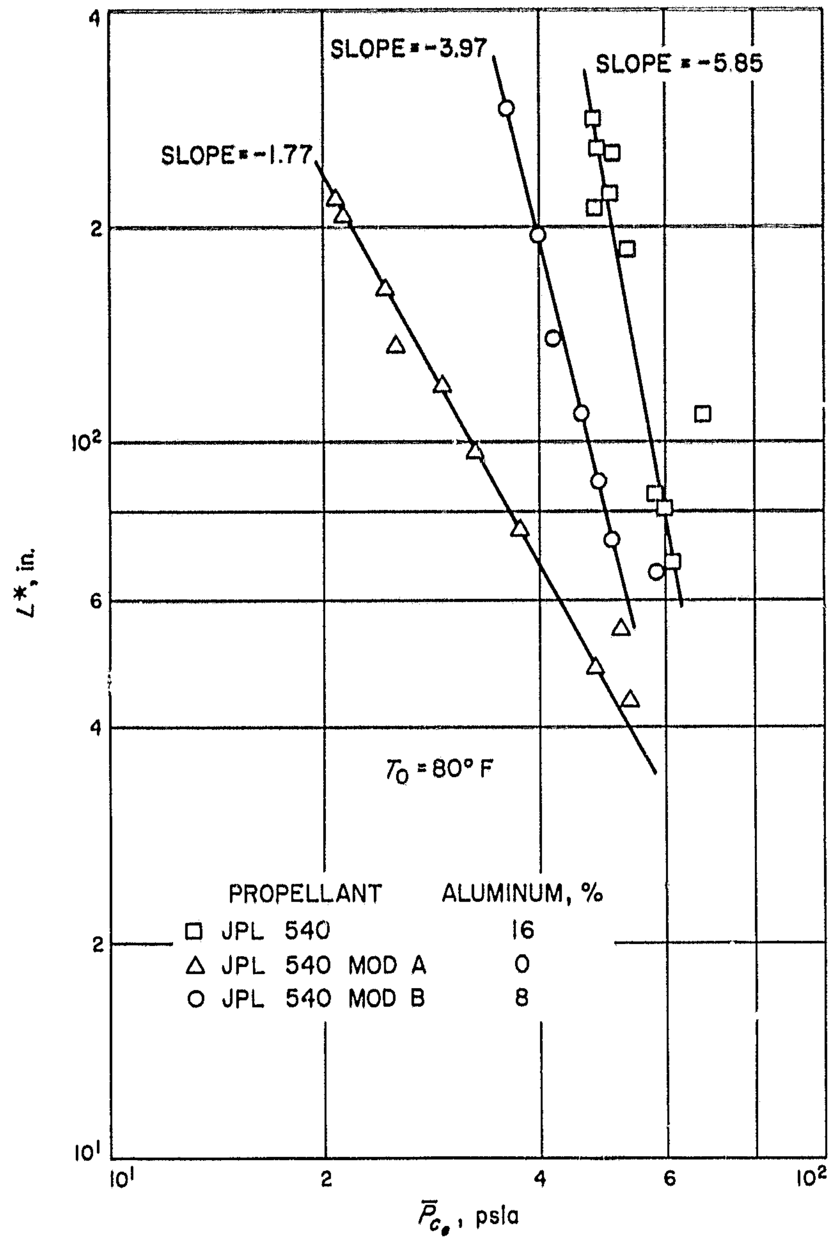

Fig. 10. L^* vs mean chamber pressure at combustion extinction, JPL 540, Mod A, and Mod B propellants

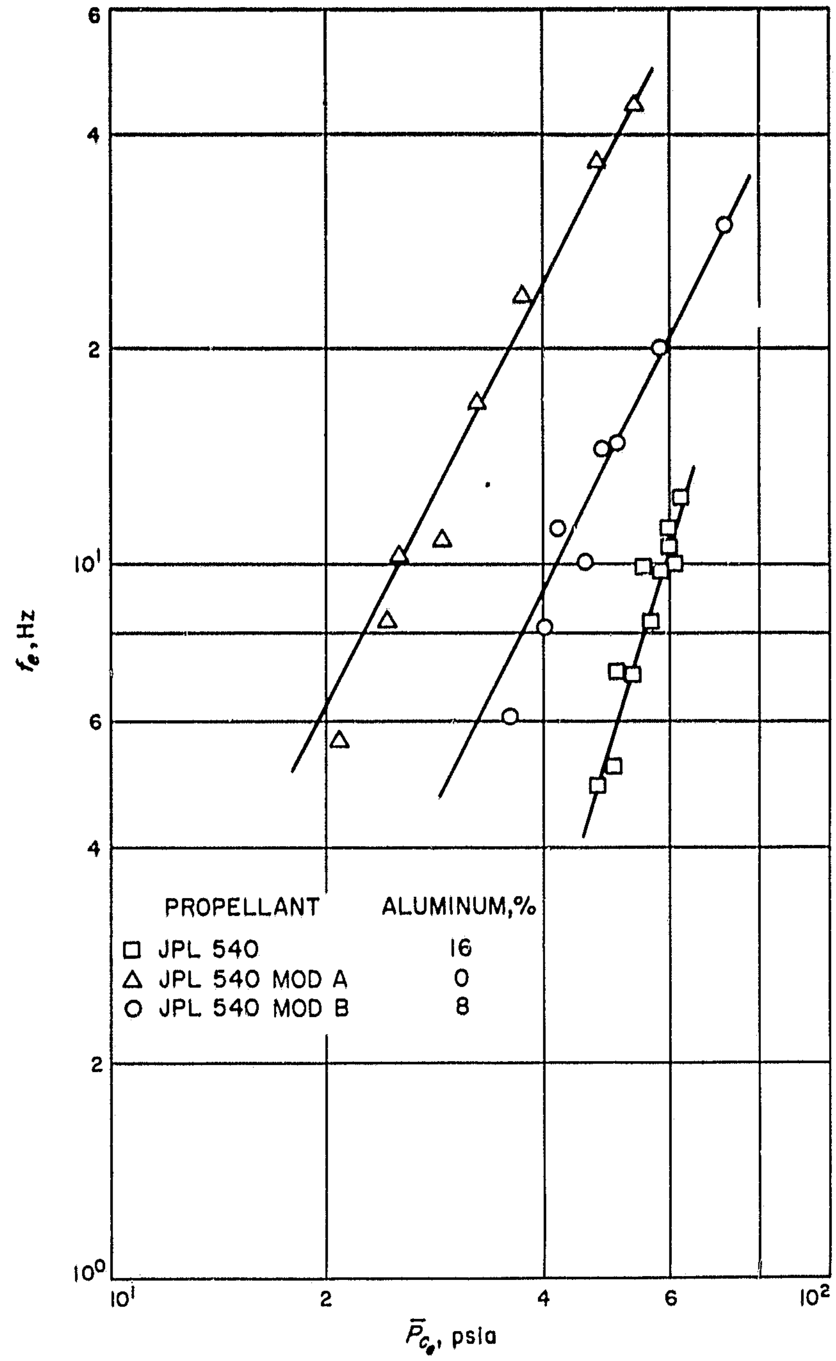

Fig. 11. Pressure oscillation frequency vs mean chamber pressure at combustion extinction, JPL 540, Mod A, and Mod B propellants

sixth propellants in Table 1, two modified versions of JPL 540 propellant (Ref. 6). The Mod 1 propellant contained aluminum with a mass median diam of 31 microns (μm), as determined by the Micromerograph particle size distribution analysis, in place of the 7-μm aluminum in the regular formulation. The aluminum additive in the Mod 2 propellant had a mass median diam of approximately 15–17 μm. Ballistic data for the two modified propellants is compared with that for JPL 540 in Figs. 13 and 14. The performance of the two propellants was nearly identical, as, will be seen, were the unstable combustion characteristics. Increasing the mass median particle size of the aluminum additive resulted in an increased low-pressure burning rate, as shown.

The extinguished propellant grains had an unusual appearance (Fig. 15), being covered with a white, flaky deposit. Chemical analysis showed the deposit to be greater than 60% unreacted aluminum. The somewhat heavier than usual slag build-up on the converging portion of the nozzle (Fig. 16) was also analyzed for percentage of free aluminum. Tests on the slag build-up for three test firings gave 30 to 40% unreacted aluminum, indicating that a good portion of the aluminum was probably passing through the motor unburned. The L^*–$\bar{P}_{c_e}$ correlations obtained for the Mod 1 and Mod 2 propellants are shown in Fig. 17, with the JPL 540 data included for comparison purposes. The data points for the two modified propellants fell on the same curve, within experimental scatter. The negative slope of the

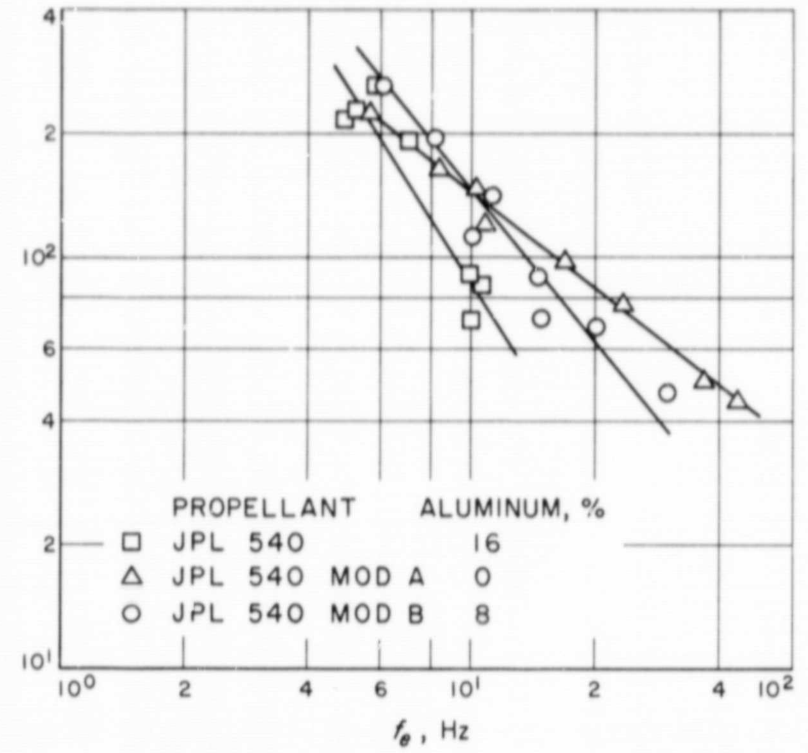

Fig. 12. L* vs pressure oscillation frequency at combustion extinction, JPL 540, Mod A, and Mod B propellants

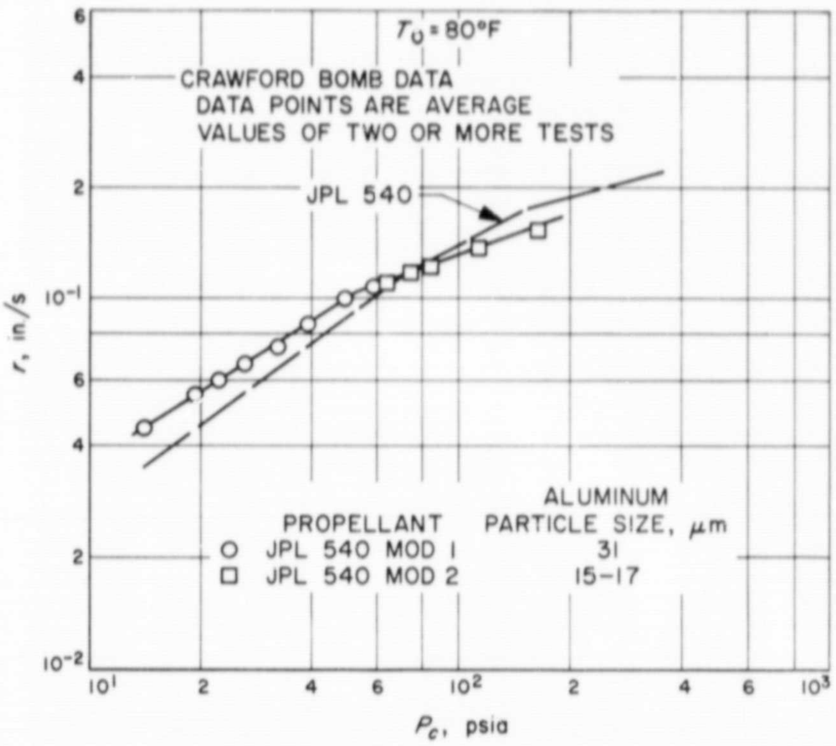

Fig. 14. Burning rate vs pressure, JPL 540 Mod 1 and Mod 2 propellants

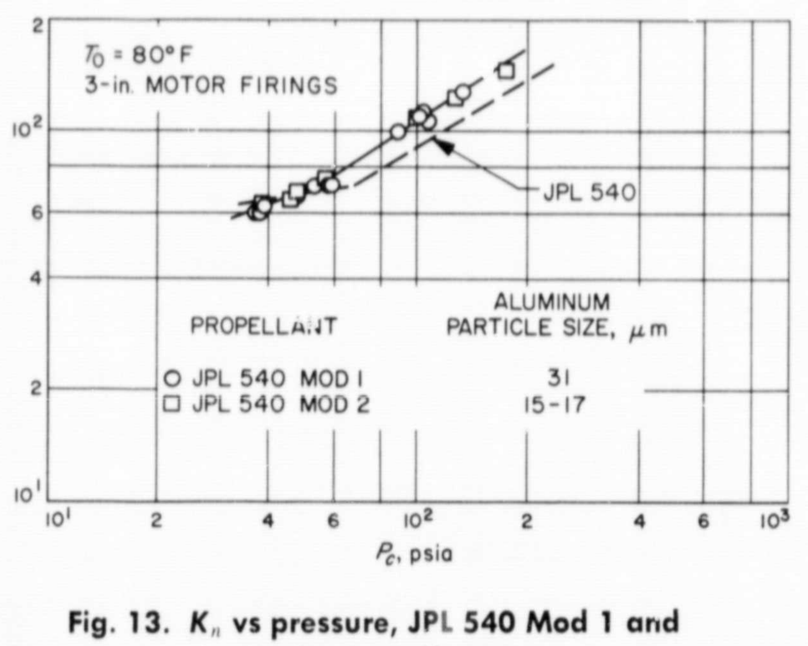

Fig. 13. K_n vs pressure, JPL 540 Mod 1 and Mod 2 propellants

curve was smaller than that for JPL 540 and laid in a lower pressure region. The pressure oscillation frequency prior to combustion extinction plotted vs $\overline{P}_{c_e}$ for the three propellants is shown in Fig. 18. Again the data points for the two modified propellants appeared to fall on the same curve. The shifts in the modified propellant ballistic and extinction curves were in the direction of the previous results for the propellants with lowered aluminum composition.

4. Oxidizer particle size. The last two modified versions of JPL 540 propellant listed in Table 1 were test

Fig. 15. Extinguished propellant grain, JPL 540 Mod 1 propellant

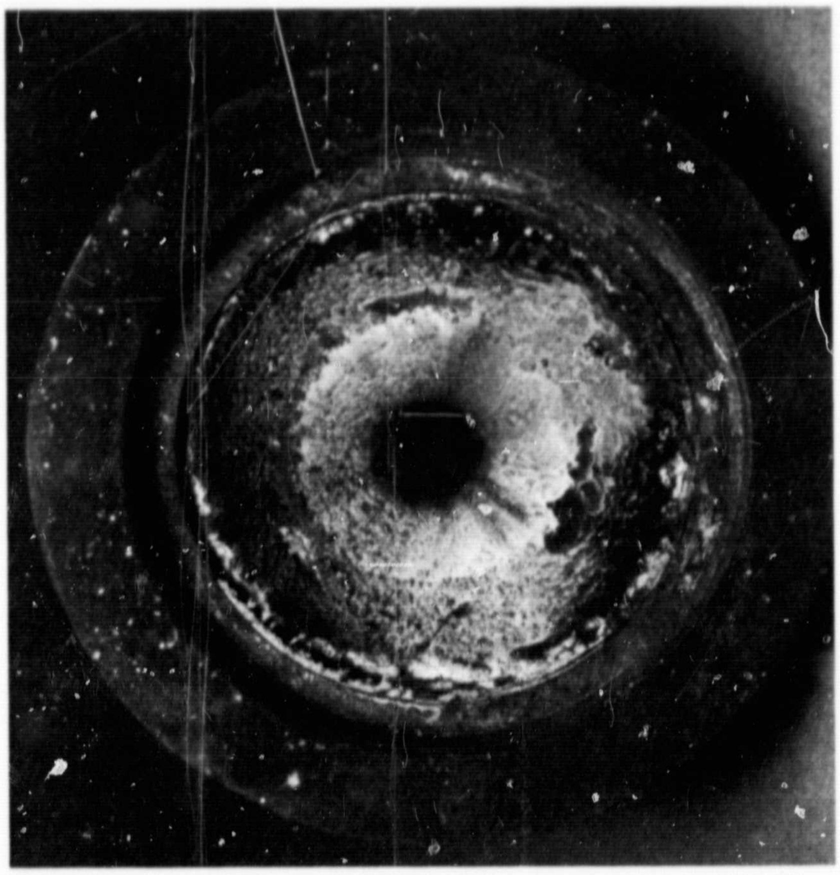

Fig. 16. Slag build-up on converging portion of nozzle, post-firing view

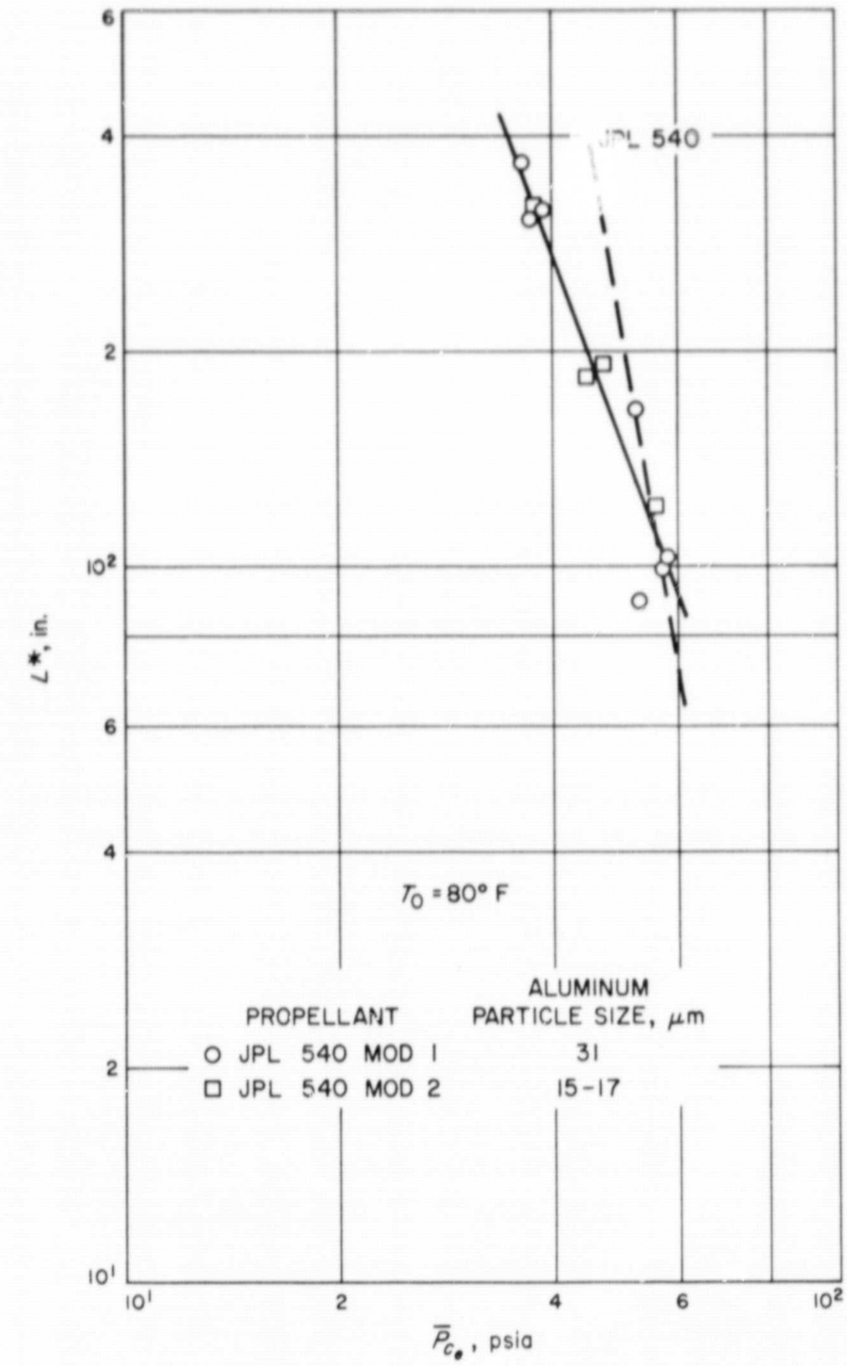

Fig. 17. L^* vs mean chamber pressure at combustion extinction, JPL 540 Mod 1 and Mod 2 propellants

fired to determine the effect of variation of the oxidizer particle size on the extinction correlation (Ref. 7). Unmodified JPL 540 uses a bimodal (70/30) oxidizer distribution, 70% unground with a mass median particle diam of approximately 170 μm and 30% ground with a 17-μm mass median diam. For the Mod 3 propellant the 70% unground oxidizer in the formulation had a 400-μm mass median diam (+48 mesh), and 31-μm aluminum was used. The Mod 4 formulation contained only the 400-μm unground oxidizer (unimodal distribution) and used the standard formulation aluminum size (7 μm). Burning rate data for these formulations and the 540 and Mod 1 propellants in the low-pressure region are shown in Fig. 19. The coarser oxidizers resulted in reduced low-pressure regression rates.

The extinction test data for the Mod 3 and 4 propellants are compared with those for the corresponding standard oxidizer propellants in Figs. 20 and 21. The modified propellants' L^*–$\overline{P}_{c_e}$ boundaries laid approximately parallel to those of the unmodified propellants, but in slightly lower pressure regions. The differences were concluded to be small, but real.

5. ***Binder type.*** Tests were also conducted to evaluate the effect of binder system on the L^*–$\overline{P}_{c_e}$ correlation (Ref. 8). The propellants tested were a United Technology Center polybutadiene-acrylic acid-acrylonitrile (PBAN) binder propellant and a Lockheed Propulsion Company nitroplastisol propellant. The test results were compared with the results of similar previously tested polyurethane (PU) binder propellants. Only a few successful tests were obtained for each of the two propellants. In the unsuccessful tests the propellant either could not be ignited or failed to extinguish until all of the propellant was consumed. From the little data that was obtained and the difficulty incurred in obtaining successful extinction tests, it was concluded that the two binder systems tested reduced the low-pressure extinction boundaries below those for their PU binder counterparts.

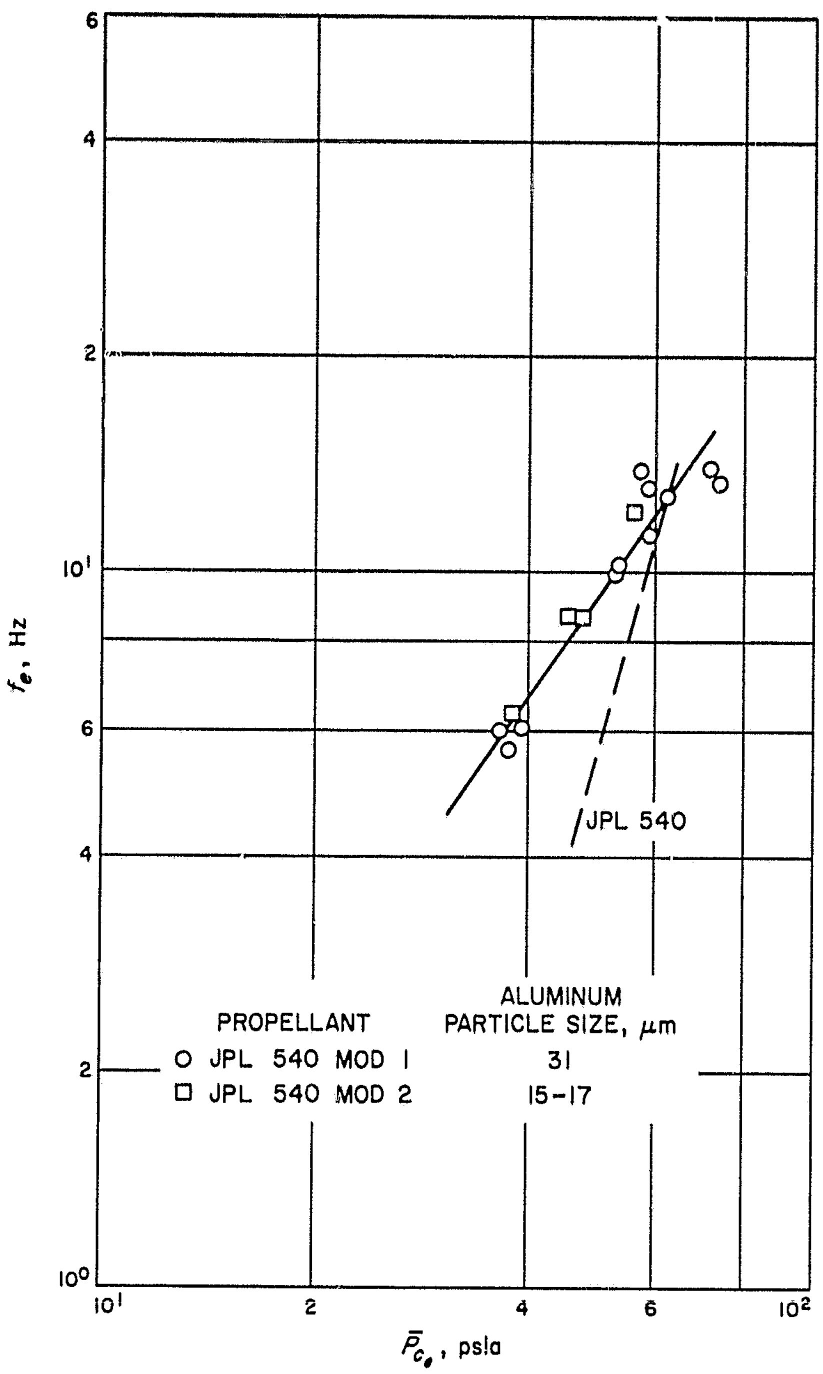

Fig. 18. Pressure oscillation frequency vs mean chamber pressure at combustion extinction, JPL 540 Mod 1 and Mod 2 propellants

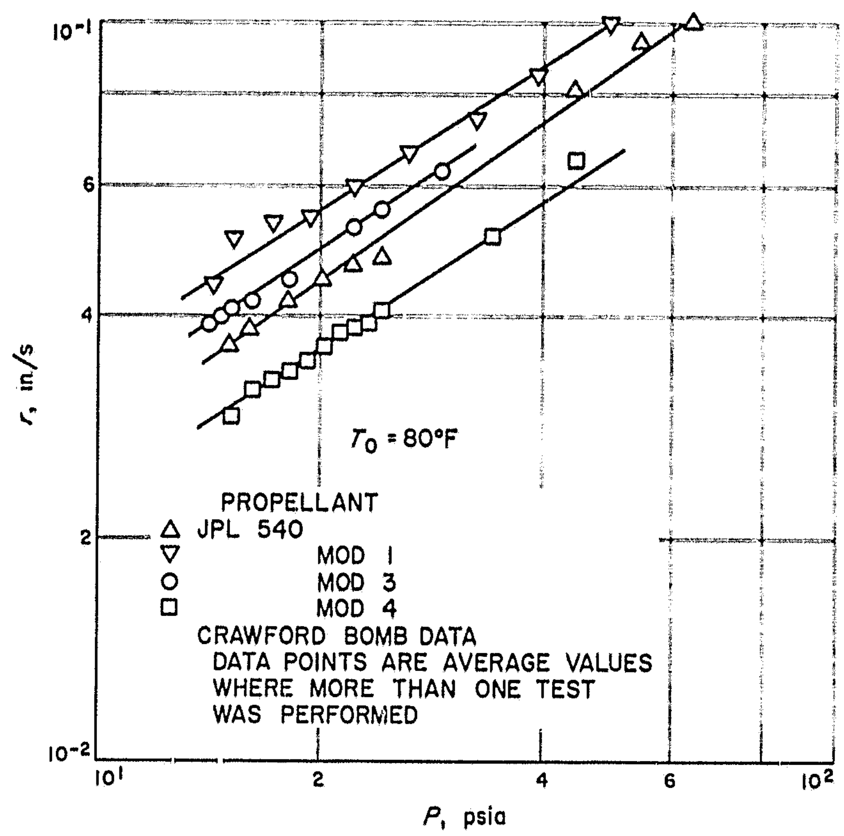

Fig. 19. Burning rate vs pressure, low-pressure region

C. Summary and Discussion

A rocket motor low-pressure stable combustion limit, in a pressure region significantly greater than the propellant's low-pressure deflagration limit, was found for each propellant tested. An L^*–$\bar{P}_{c_e}$ correlation was found to be a valid parameter for portraying this combustion limit.

The slope of the L^*–$\bar{P}_{c_e}$ relationship was affected by the presence of aluminum, the concentration of aluminum, and the particle size (coarseness) of the aluminum in the propellant. The effect of increased aluminum coarseness appeared to be the result of modifications to the aluminum melting or combustion processes (Fig. 15), as the burning and extinction characteristics approached those of a non-aluminized propellant.

Coarser oxidizer propellants had a slightly greater resistance to low-pressure extinction (extinction occurred at a lower pressure for a given L^*), in spite of their reduced burning rates. This may possibly be due to the greater heat retention capacity (lower surface-to-volume ratio) of the larger oxidizer granules.

The PBAN and nitroplastisol propellants tested were more difficult to extinguish than similar PU propellants. As has been pointed out (Ref. 9), this is probably due to differing binder degradation processes.

A trend was observed between ease of extinguishment and propellant burning rate. Generally, the greater the low-pressure burning rate of a propellant, the lower were the motor L^*s and pressures required before combustion instability and extinction would occur. A notable exception to this is seen in the test results for the 534 and 540 Mod A propellants. A comparison of Figs. 5 and 10 shows the extinction characteristics to be essentially identical, although the catalyzed 534 propellant has a significantly higher low-pressure burning rate.

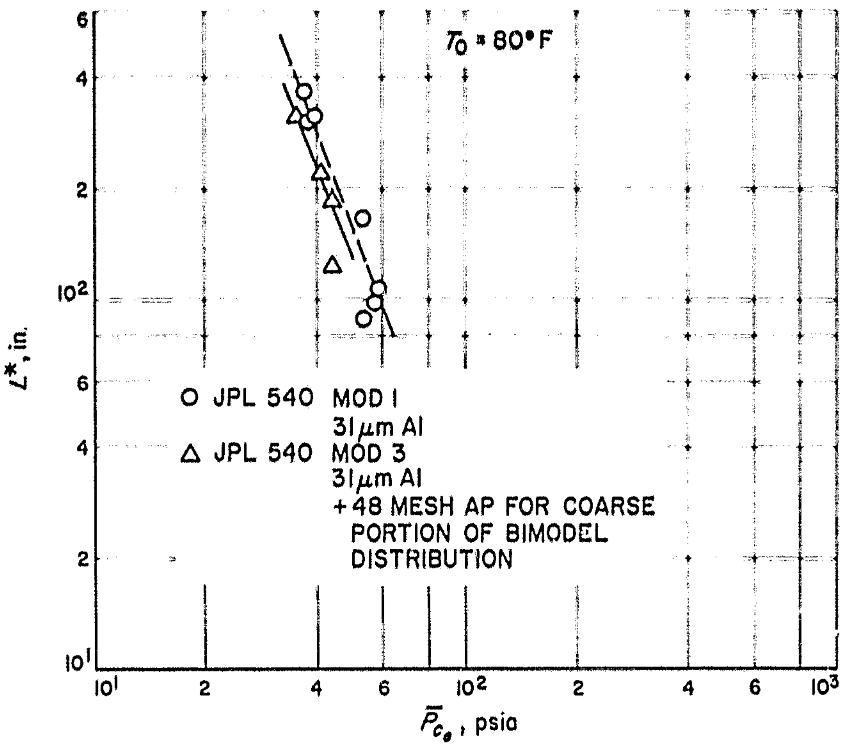

Fig. 20. L^* vs mean chamber pressure at combustion extinction, JPL 540 Mod 1 and Mod 3 propellants

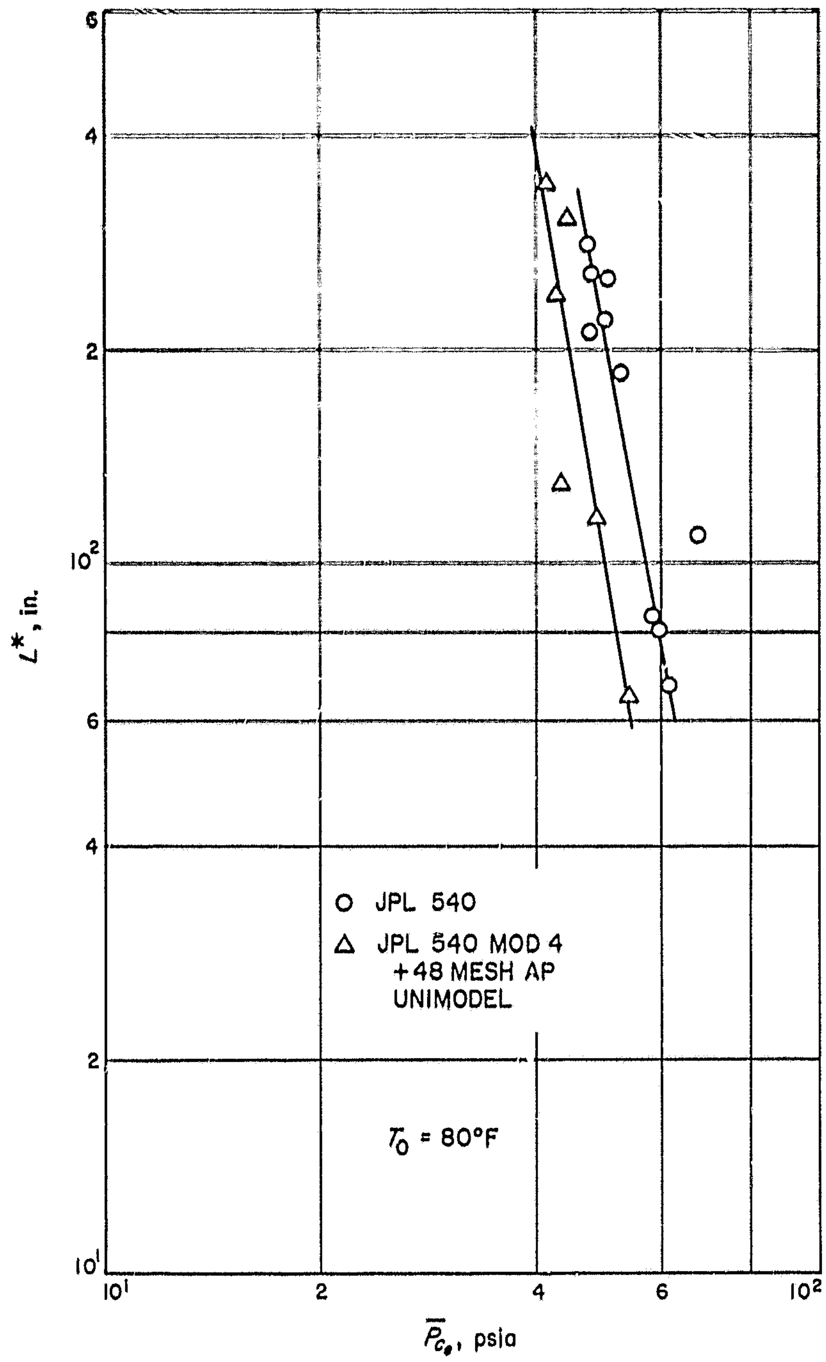

Fig. 21. L^* vs mean chamber pressure at combustion extinction, JPL 540 and 540 Mod 4 propellants

III. Transparent Motor Tests

In an attempt to obtain a better understanding of the actual mechanisms causing low-pressure extinction, a transparent solid rocket motor was designed that permitted propellant charge surfaces to be photographed while burning regressively into the unstable pressure region.

A. Test Equipment

The transparent motor was basically the motor of Fig. 1 with a 6-in.-long, ¼-in.-wall-thickness Lucite chamber substituted for the steel one (Fig. 22). A new Lucite chamber was used for each test firing. Regular cylindrical regressive propellant charges were used in the motor, as well as the usual pressure measurement instrumentation.

Two high-speed motion picture cameras, a Fastax and a Fairchild 16, recorded the propellant firings. Ektachrome ER 430 Daylight film was used in both cameras with 500- and 1000-Hz timing marks placed on the film. No lighting other than the illumination from the motor itself was used. Firings were made using narrow-band filters, neutral density filters, and no filters on the cameras. The latter proved most satisfactory for photographing all propellants except one containing copper chromite (dark blue emission), and no filters were used for a majority of the tests.

B. Test Procedure

The Fastax camera, used with a 50-mm lens and operating at 1000 fps, photographed the overall burning grain. The Fairchild 16, operating at 4000 fps, was focused on a small portion of the propellant surface. After much experimenting the combination of a 6-in. lens and 2-in. extension tube was settled on as the best compromise for the Fairchild camera, giving approximately a ¾-in., square, focal plane, with an adequate depth or field. The closeup camera was usually focused normal

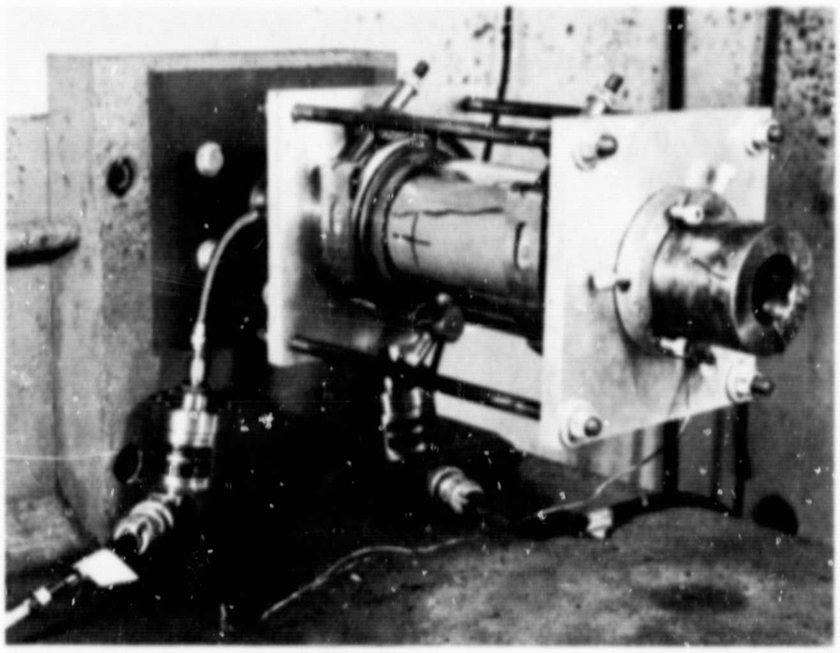

Fig. 22. Transparent motor with dummy charge, mounted on test stand

to the propellant surface at about where the square mark is located in Fig. 22, or raised slightly to photograph along the upper edge of the grain.

A correlation blip was placed on the film and the oscillograph pressure/time trace after the propellant had ignited and the cameras accelerated up to speed, enabling the film and pressure traces to be matched later over the entire test run.

The tests were designed so that low-pressure extinction occurred about 2–4 s following ignition, within the visual and structural lifetime of the Lucite chamber. Since the tests were performed under atmospheric conditions, in all but a few of the test firings the propellant charges reignited several seconds after extinction and chuffed until all of the propellant was consumed.

C. Results

Motor firings were conducted using the first, second, and fifth propellants in Table 1 (JPL 534, 540, and 540 Mod 1). A qualitative picture of the low pressure (< 100 psia) combustion of the aluminum propellant additive was evident from the motion picture records. The aluminum appeared to melt on the propellant surface, agglomerate, rise into the hot gas stream as large droplets, and ignite.

It was difficult to detect from the films any variation in the rate or magnitude of the efflux of aluminum from the propellant surface throughout the low-amplitude pressure oscillations (2–6 psi) of the 540 propellant. The efflux appeared steady and random right up to combustion extinction. The much higher amplitude oscillations obtained during some tests with the Mod 1 propellant were accompanied by significant variations in light intensity and the amount of aluminum efflux throughout the oscillation cycle.

Motion picture film and oscillograph pressure data were correlated for several test firings. Common characteristics of the motion picture films and pressure data gave an indication of the series of events leading to complete combustion extinction. These events consisted of (1) the onset of extinction, (2) a rapid decrease in propellant gasification, (3) extinction, and (4) chamber venting. The location of these events on a typical oscillograph pressure/time trace is shown in Fig. 23. On the film, the onset of extinction B was a break and rapid decrease in the light intensity; at Point D, gasification appeared to begin to decrease, with darkening of frames; and at extinction E_x, gasification appeared to have largely ceased.

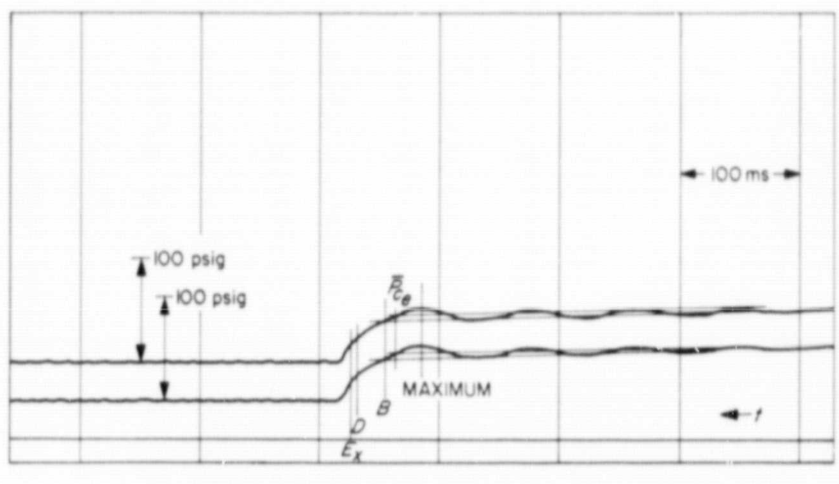

Fig. 23. Pressure/time trace for Run 1491, JPL 540 Mod 1 propellant

In all of the tests analyzed the point on the pressure trace at the onset of extinction B fell on, or very close to, the intercept point of a curve drawn through the minimum or base points of the pressure oscillation cycles preceding extinction (Fig. 23). To explore this further, this intercept pressure value was measured from the data record for each of the JPL 540 Mod B tests. The results, again plotted logarithmically vs the extinction L^* values, are compared with the previously determined mean pressure curve for Mod B in Fig. 24. A curve fit to the data fell approximately parallel to and 5 to 7 psi below

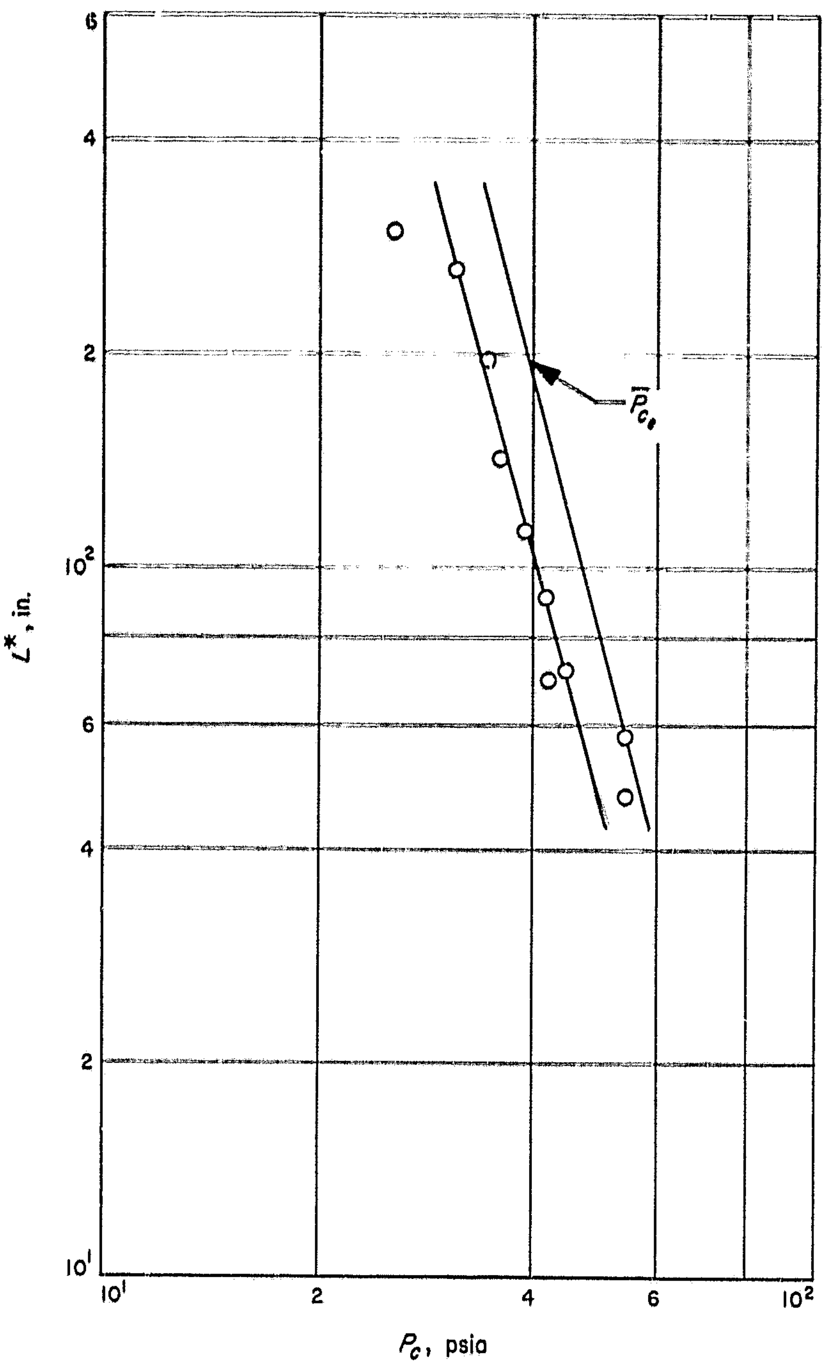

Fig. 24. L^* vs base pressure curve intercept point at combustion extinction, JPL 540 Mod B propellant

the higher mean pressure curve. Similar results would be expected for the other propellants tested.

IV. Additional Data Reduction

In an attempt to gain further insight into the actual mechanisms of low-pressure instability and extinction, additional reduction and analysis of the previously described test data was pursued.

A. Onset of Instability

The motor L^* and chamber pressure at the onset of instability (OI) were determined for the first four propellants listed in Table 1. The onset point was defined as the point of initiation of the chamber pressure oscillations that continued to increase in amplitude until combustion extinction occurred (Fig. 25). The P_c values were measured from the oscillograph traces. The L^* values were obtained by (1) determining the propellant burning area at OI from experimentally determined K_n (burning area to throat area ratio) $-P_c$ graphs, (2) calculating the propellant charge dimensions at OI by back-calculating from the measurements taken at extinction, and (3) calculating the propellant volume and consequently motor L^*. For all propellants analyzed the OI boundary, plotted as the usual L^*–P_c log–log graph, laid approximately parallel to and to the right (higher pressure regime) of the extinction boundary, as expected from test experience. The onset of instability and extinction boundaries for the 0, 2, 8, and 16% aluminum propellants are shown in Figs. 26–29. The OI boundary approached the extinction boundary with decreasing propellant aluminum/oxidizer concentration ratio.

A possible mechanism for this low-pressure, low-frequency instability was discussed in Ref. 4. The observed pressure oscillations were felt to be a resonance phenomenon related to the characteristic exhaust time of the chamber. Instability occurred in the rocket dynamic flow system when the characteristic time of propellant burning-rate overshoot (response time) for a slight pressure fluctuation approached the characteristic exhaust time of the rocket chamber. The characteristic time for such a burning-rate overshoot phenomenon was shown in Ref. 10 to be a function of the steady combustion pressure, increasing with decreasing pressure. A transient mass balance for a solid rocket shows the characteristic response time of the exhaust process to a perturbation in chamber pressure to be simply related to L^* and essentially independent of the rocket chamber pressure level. In the test firings the onset of instability therefore occurred when the motor pressure decreased to the point where the system became dynamically unstable.

A theoretical analysis based on this model for dynamic instability was put forth in Ref. 11. This analysis, extending the original work of Akiba and Tanno (Ref. 5), attempted to predict the onset of instability for a given propellant. A highly simplified propellant combustion model, consisting of a 1-dimensional, homogenous-type propellant with all exothermic reactions occurring in a gaseous combustion zone located above the propellant surface, was used. An instability analysis of a closed-loop model for the previously described rocket dynamic

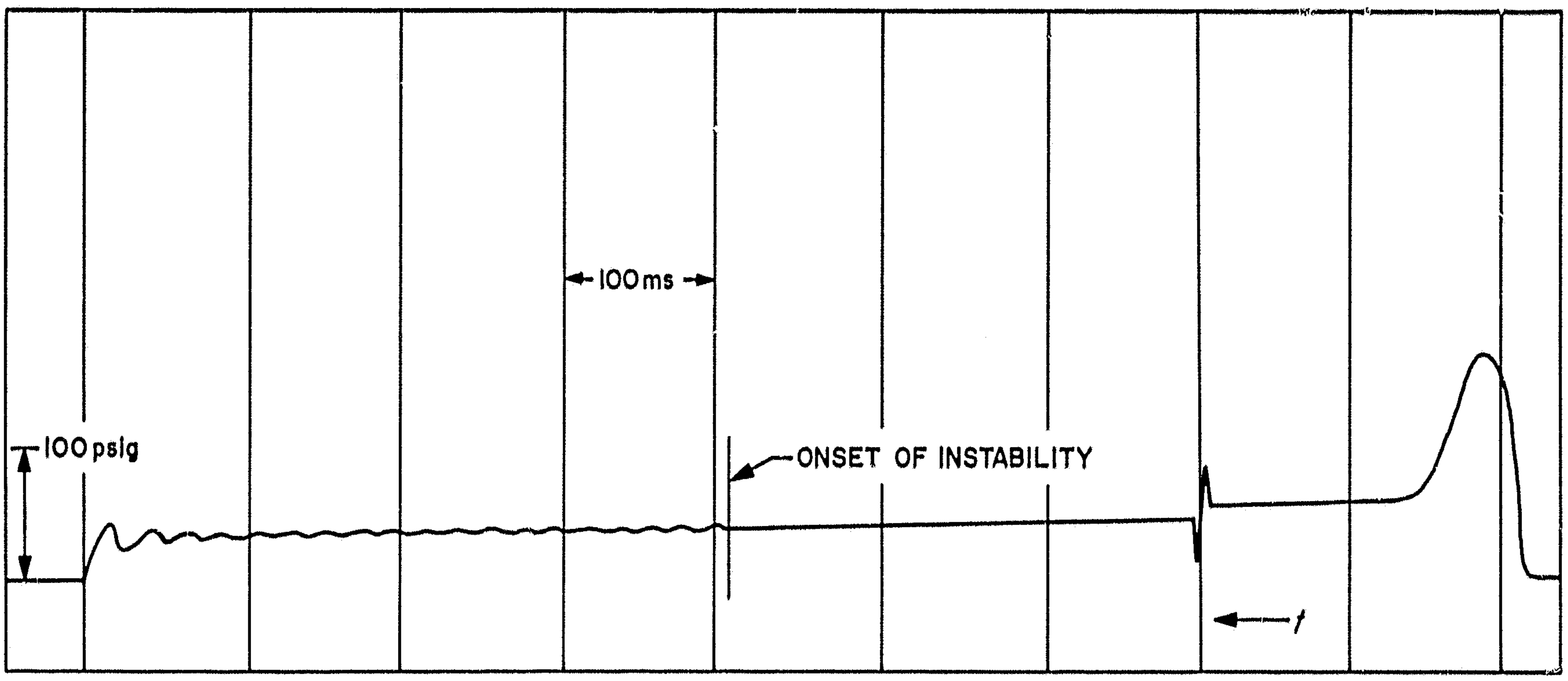

Fig. 25. Pressure/time trace for Run 1468, JPL 534 propellant

system resulted in the following L^* vs $\bar{P}_c$ instability boundary correlation:

$$L^* = \left[\frac{4\,(\tau_n)_{cr}\,\alpha\, C_D\, RT}{M\, a^2}\right] \bar{P}_c^{\,2n} \qquad (1)$$

where $(\tau_n)_{cr}$ is the critical value for conditional stability of the nondimensionalized chamber time constant, a function of the propellant's combustion model parameters: mean surface temperature, Arrhenius relationship exponential term, energy of decomposition, burning rate pressure exponent n, and solid phase constant pressure specific heat. The above correlation, plotted on log-log coordinates, has a slope equal to twice the burning rate pressure exponent.

Comparison of the theory with experimental *extinction* data for the 2% aluminized propellant (assuming the stability and extinction boundaries to be identical), using the best available values for the chemical parameters, yielded order of magnitude agreement only (Fig. 30).

The experimental onset-of-instability slope values for the non-aluminized and weakly aluminized propellants (Figs. 26 and 27) are in good agreement with the theory, whereas the experimental negative slopes for the two significantly aluminized propellants (Figs. 28 and 29) are considerably greater than predicted theoretically. This latter result is not too surprising, since the highly complex combustion of the aluminum additive was not considered in the simplified theoretical combustion model.

Investigators (Refs. 12 and 13) have reported propellant strand burning experiments where the intermittent accumulation and burning of the aluminum component was observed, with periods comparable to those occurring for low-frequency combustion instability. The resulting pressure perturbations that would occur within a rocket motor could certainly initiate and amplify (Ref. 14) the coupled combustion-mass discharge type of instability.

The subject of non-acoustic combustion instability has since been treated analytically by a number of authors (Refs. 15–20). The last four papers have applied acoustic combustion instability theory to non-acoustic instability, and, although complete agreement with available experiment data is still lacking, the phenomenon is believed to be fairly well understood.

B. Pressure Oscillation Rate of Depressurization at Extinction

Study of the low-pressure extinction test oscillograph records indicated that, as a result of the increasing amplitude of pressure oscillations following the onset of instability, the rate of depressurization of the oscillations increased up to the point of extinction. Because of the

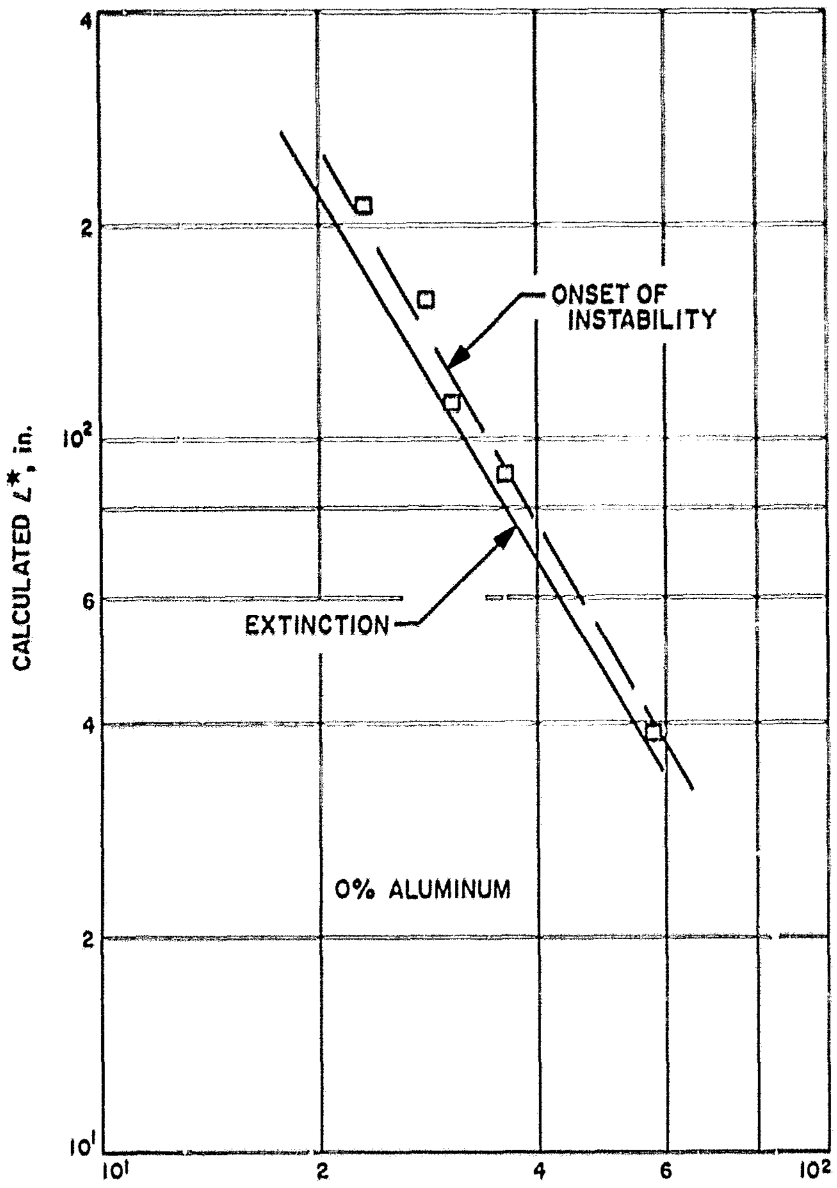

Fig. 26. L^* vs chamber pressure at onset of instability, JPL 540 Mod A propellant

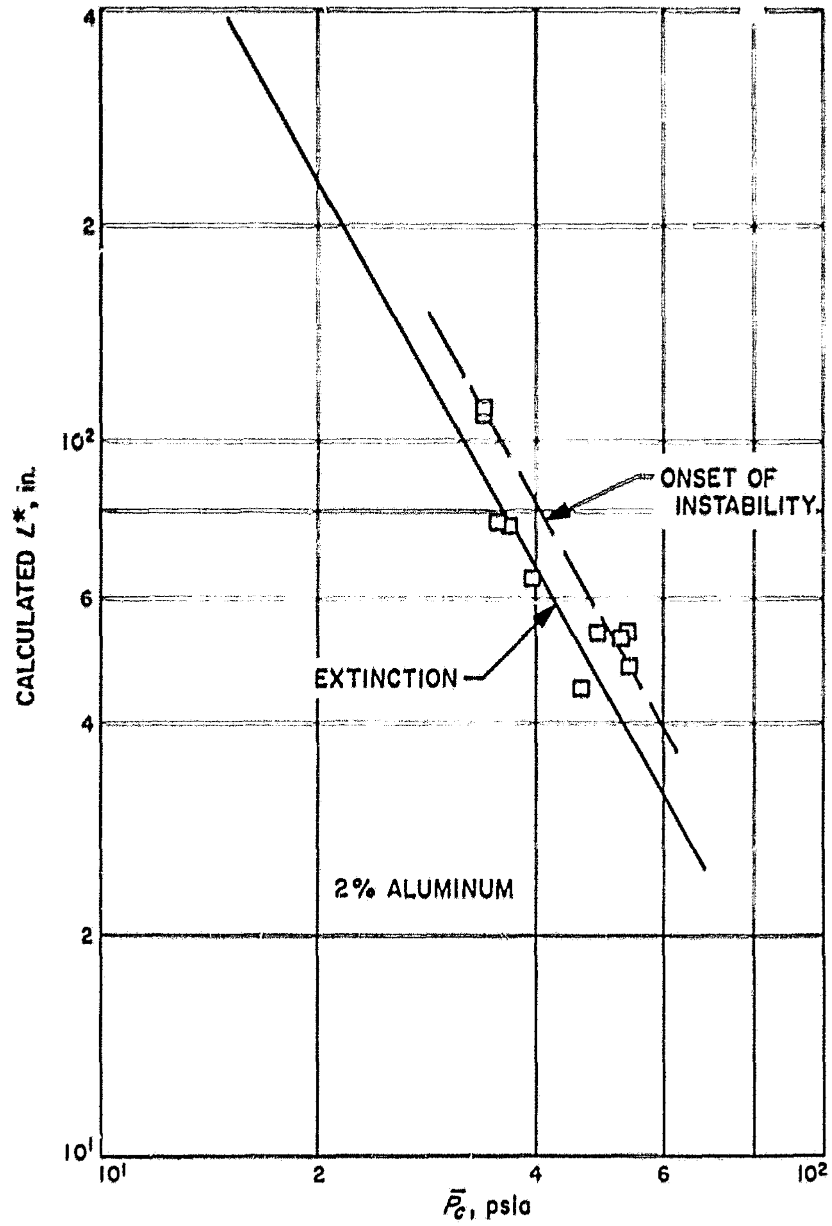

Fig. 27. L^* vs chamber pressure at onset of instability, JPL 534 propellant

higher frequencies of pressure oscillation for the nonaluminized propellants, the corresponding depressurization rates also appeared to be of greater magnitude. The possible significance of pressure perturbations on extinction had been noted earlier by Cohen (Ref. 21). From the oscillograph data the negative slope of the last pressure oscillation at or immediately prior to the onset of extinction was therefore measured (at best a very approximate measurement) for JPL 540 propellant and the first four modification propellants in Table 1, as shown in Fig. 31. Although there was a great amount of scatter in the data, a definite correlation between the rate of depressurization $(dP/dt)_e$ and the mean chamber pressure prior to extinction $(\bar{P}_{c_e})$ was found for each propellant (Fig. 32). For each propellant the correlation crossed the pressure coordinate $[(dP/dt)_e = 0]$ at a pressure significantly greater than the measured deflagration limit of the propellant (Figs. 33 and 34), thus indicating the existence of a minimum pressure below which stable combustion within a motor cannot occur. This minimum pressure increased with increasing aluminum/oxidizer concentration ratio.

C. Frequency of Oscillations and Rate of Depressurization vs Pressure

The data presented in Figs. 11 and 18 showed that, under low-frequency instability conditions, a correlation existed between the frequency of pressure oscillations and the mean chamber pressure at combustion extinction. In order to assess the importance of the pressure oscillation rate of depressurization on low-pressure combustion extinction, it was deemed necessary to determine if the

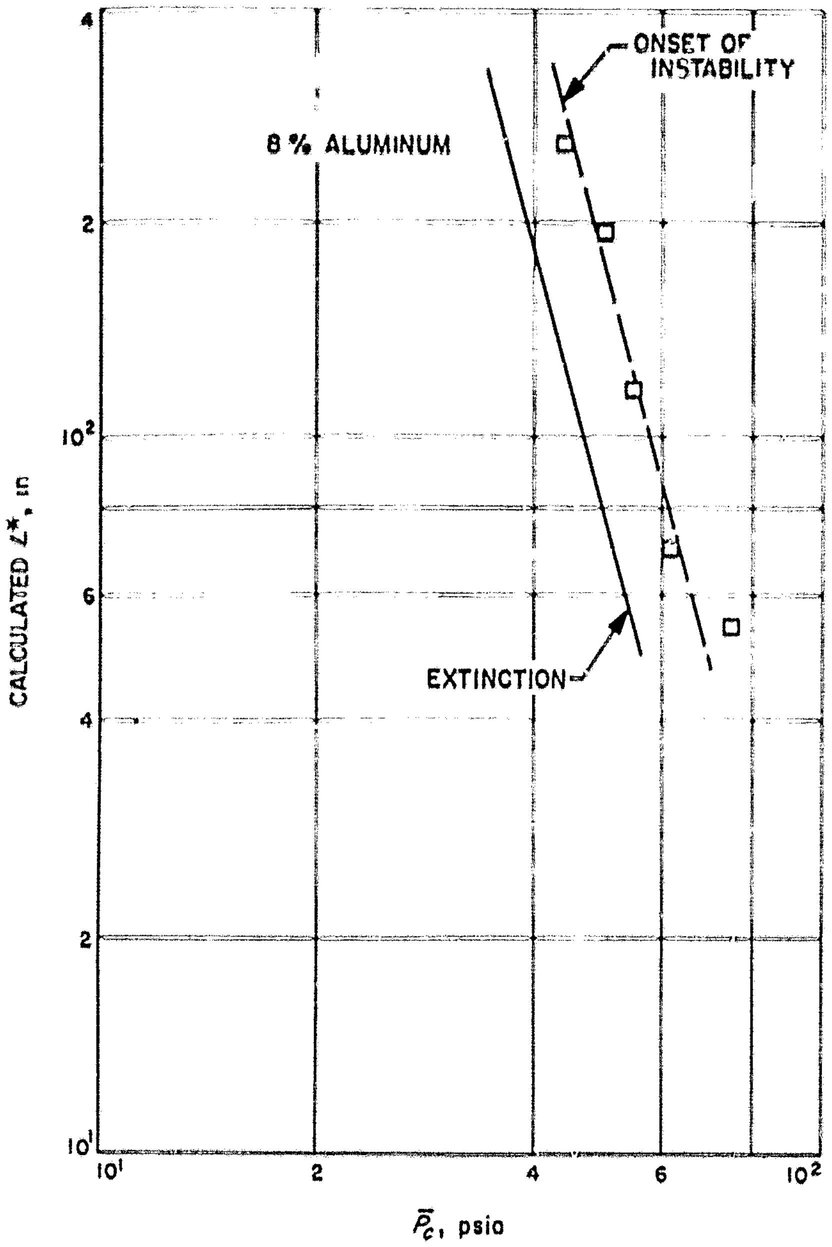

Fig. 28. L^* vs chamber pressure at onset of instability, JPL 540 Mod B propellant

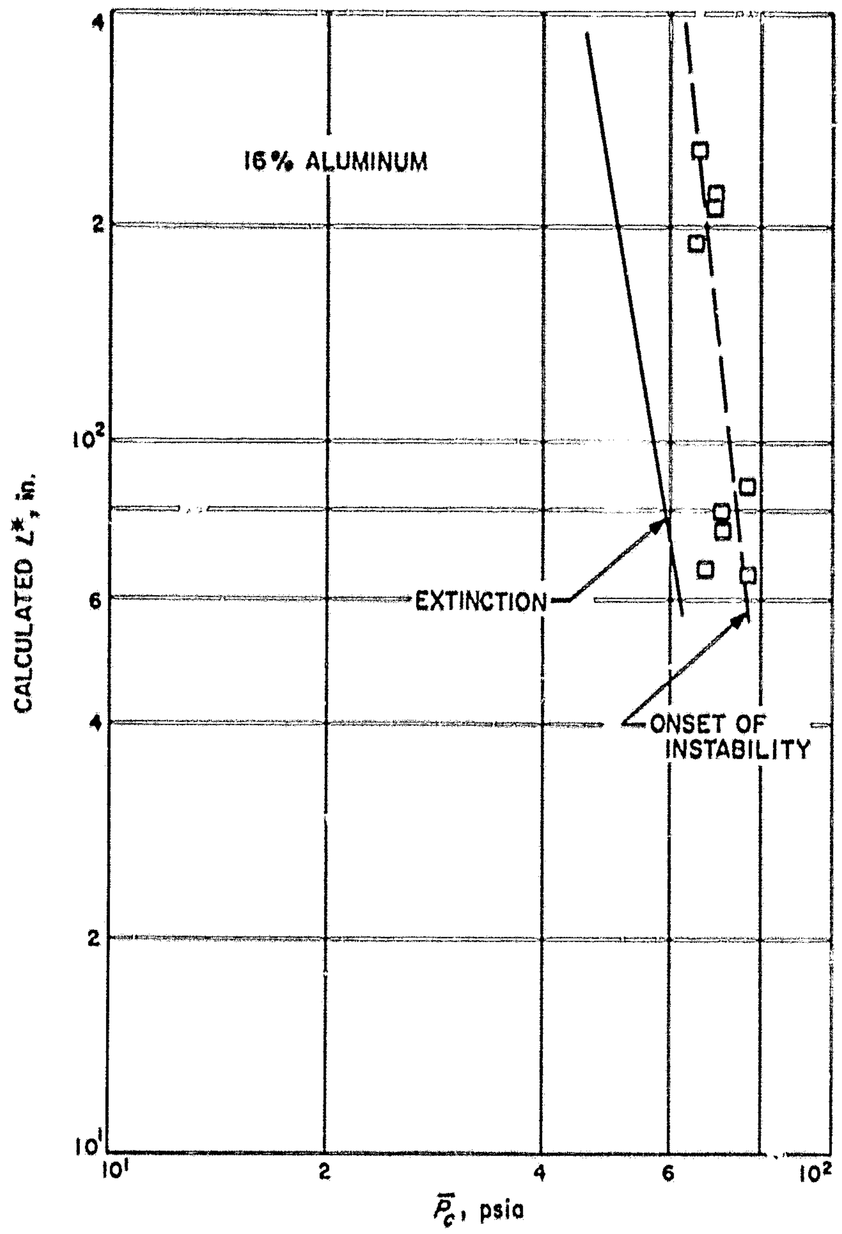

Fig. 29. L^* vs chamber pressure at onset of instability, JPL 540 propellant

rate-of-depressurization–pressure correlation at combustion extinction described in the previous section was significant in itself, or was merely a consequence of the correlation between frequency and pressure.

Further data reduction was therefore performed on the test data records for the same five propellants used in the previous section. The additional information consisted of the mean chamber pressure, motor L^*, frequency of pressure oscillations, and pressure oscillation maximum rate of depressurization at various points on the test oscillograph pressure–time traces prior to the occurrence of extinction.

Figure 35 is a log–log plot of the frequency of pressure oscillations plotted versus the mean chamber pressure for several test firings with the non-aluminized propellant. The frequency data correlated fairly well with pressure, in good agreement in the same pressure region with the results of tests with similar propellants reported by NWC (Ref. 12). Plotting the maximum rate of depressurization of the pressure oscillations logarithmically versus chamber pressure for the same test runs (Fig. 36), only the extinction depressurization points correlated with pressure. Figures 37–42 show the same type of data for the 8%, 16%, and coarser-grade 16% aluminized propellants respectively. Similar results were obtained.

The conclusion reached was that this difference in the character of the frequency and depressurization rate correlations with pressure seemed to substantiate the significance of the pressure oscillation rate-of-depressurization–pressure correlation at extinction itself.

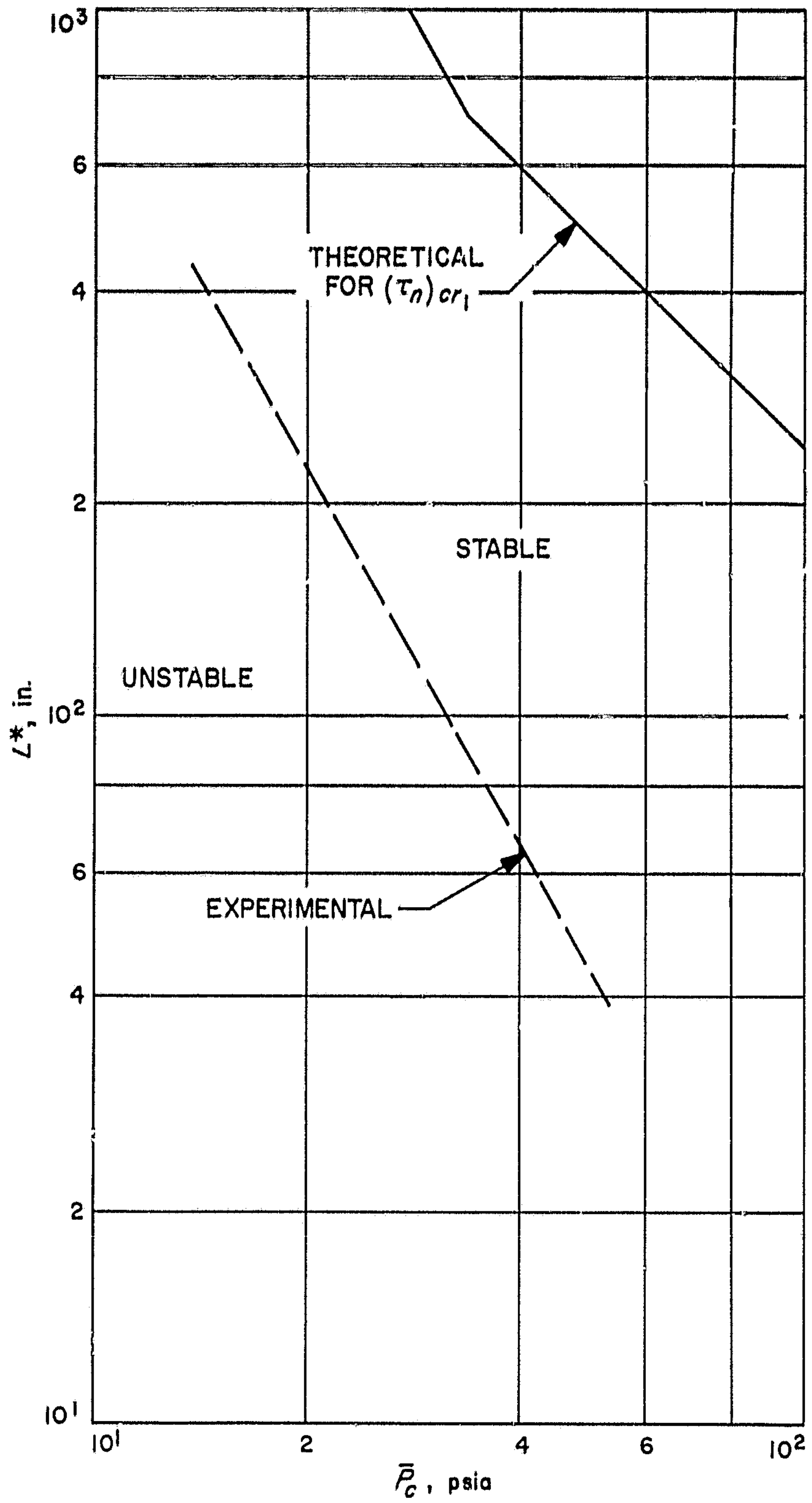

Fig. 30. L^* vs extinction pressure relationship for JPL 534 propellant

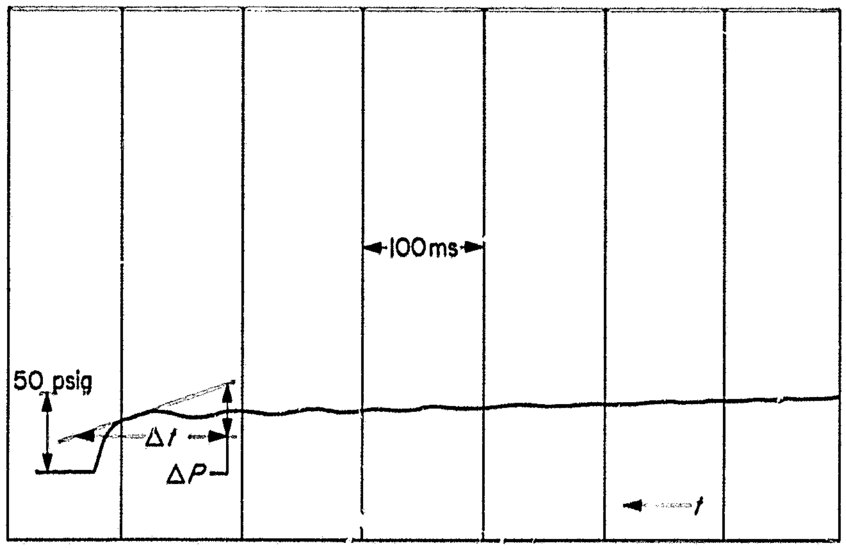

Fig. 31. Pressure/time trace for Run 1437, JPL 540 Mod B propellant

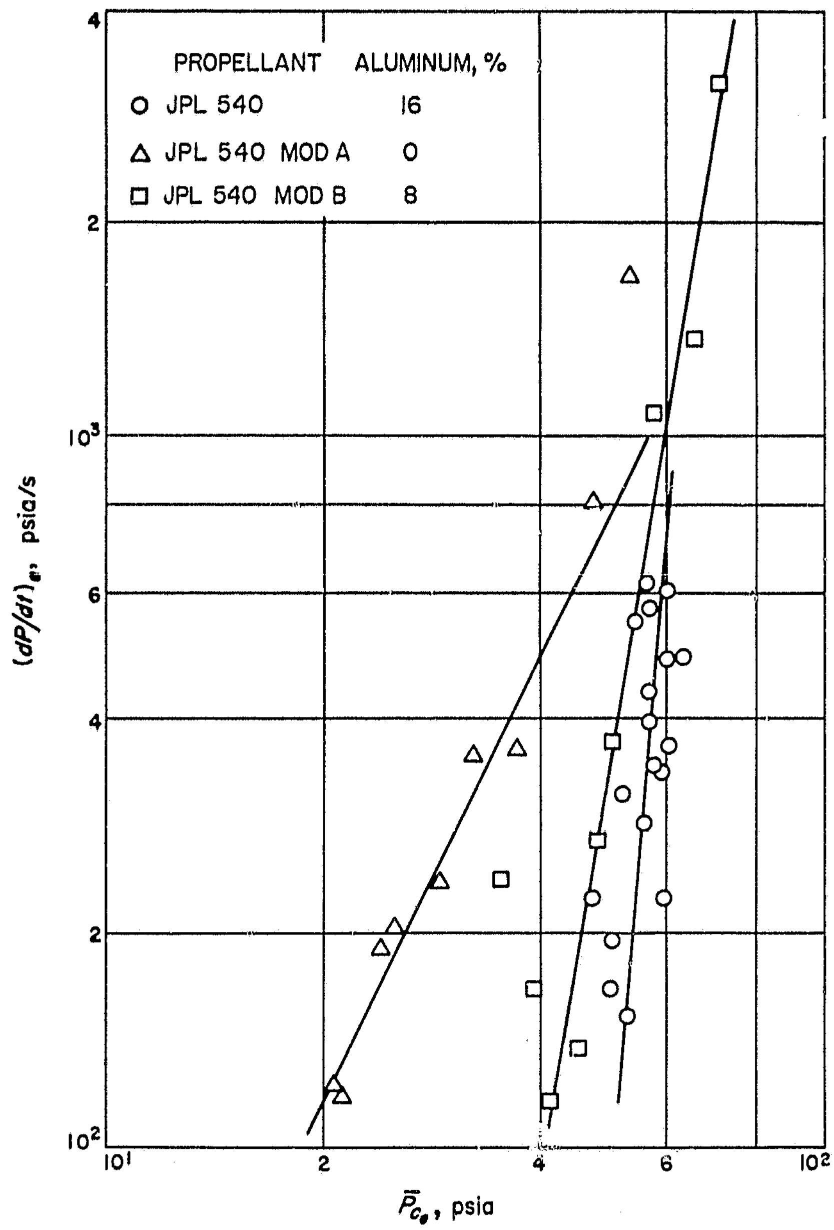

Fig. 32. Rate of chamber depressurization vs mean chamber pressure at combustion extinction, log–log plot

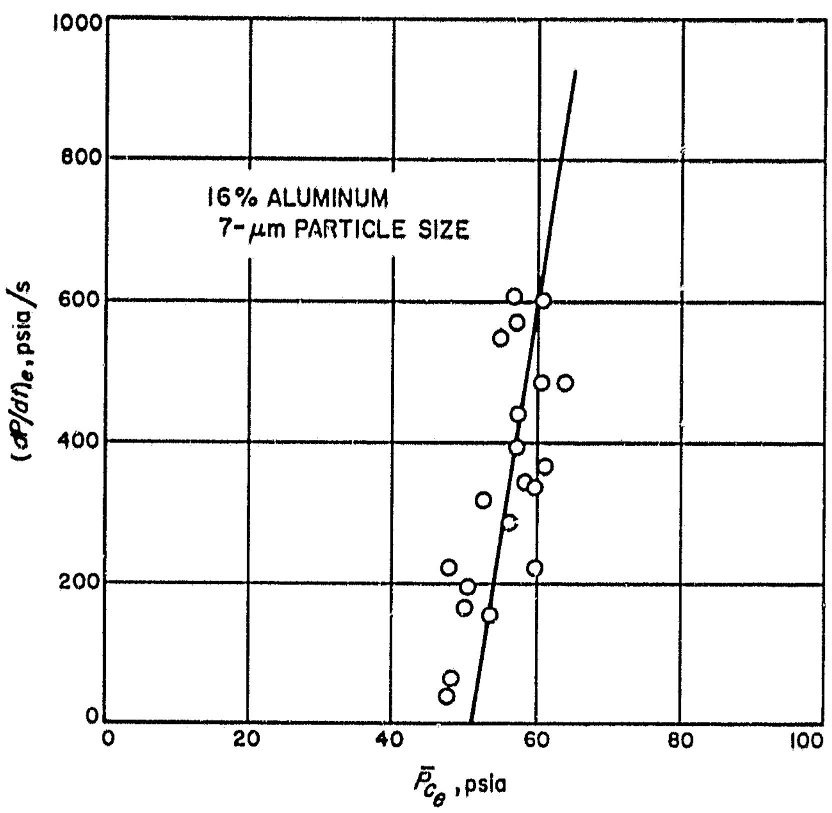

Fig. 33. Rate of chamber depressurization vs mean chamber pressure at combustion extinction, JPL 540 propellant

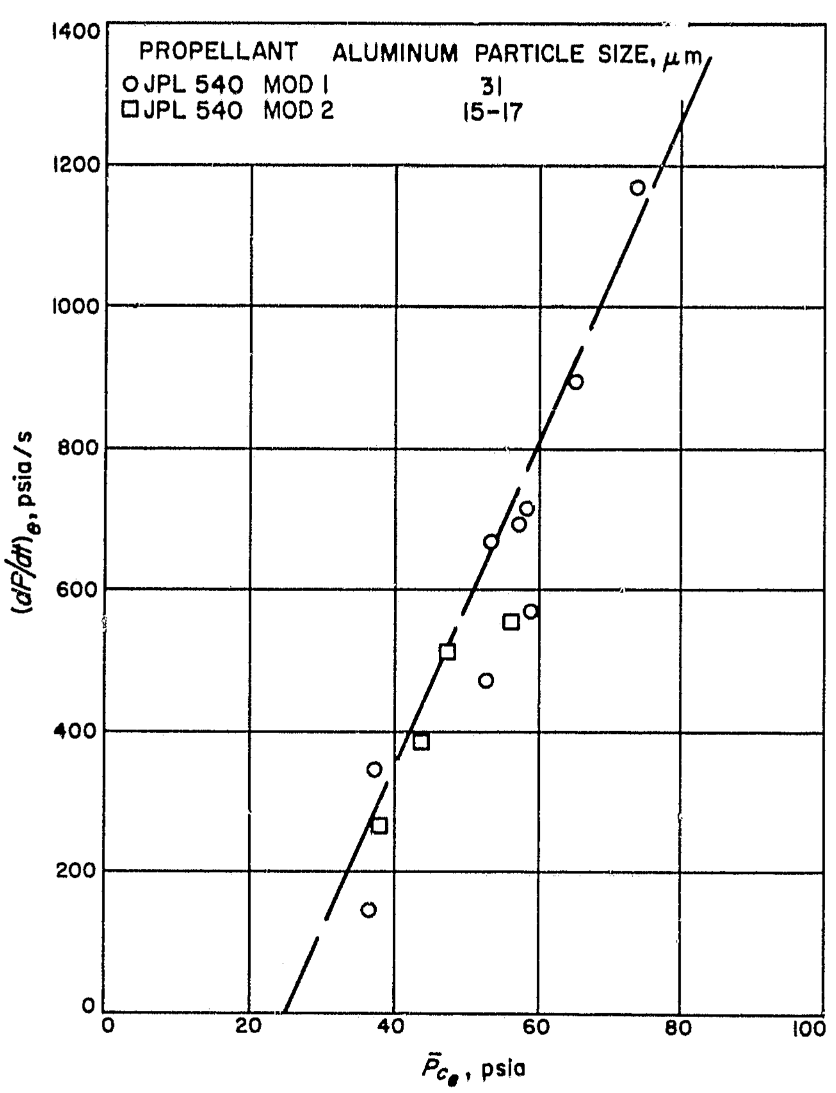

Fig. 34. Rate of chamber depressurization vs mean chamber pressure at combustion extinction, JPL 540 Mod 1 and Mod 2 propellants

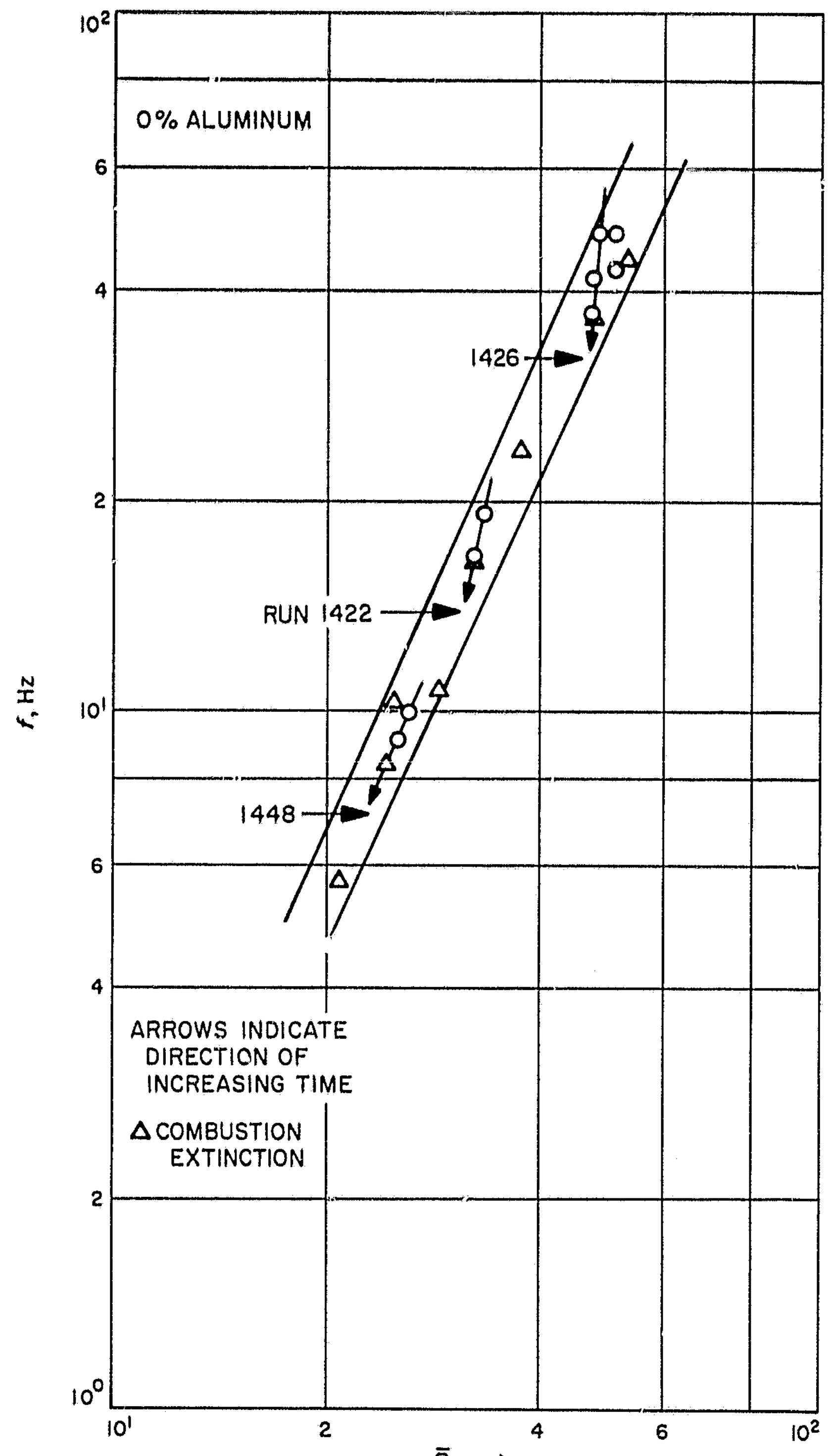

Fig. 35. Pressure oscillation frequency vs mean chamber pressure, JPL 540 Mod A propellant

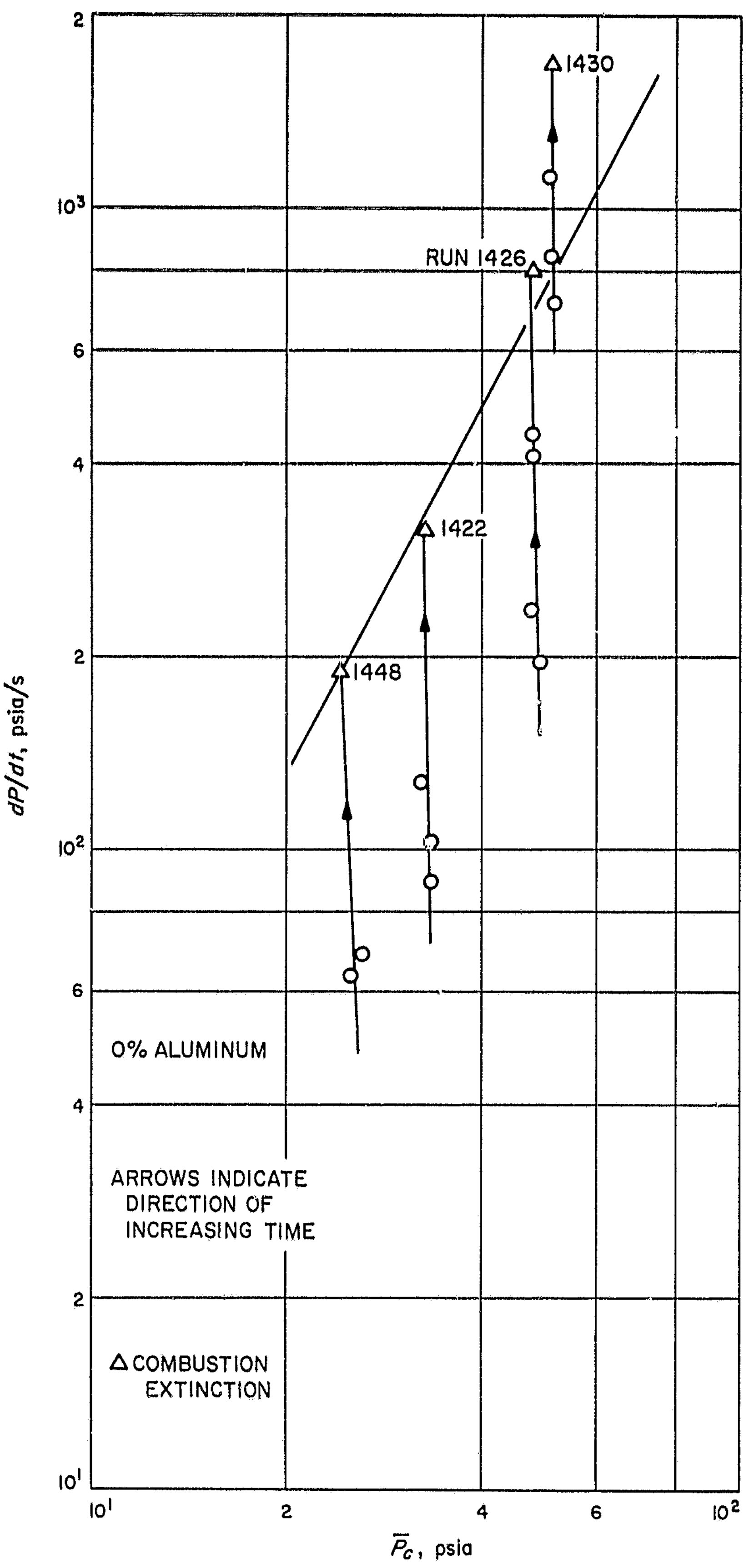

Fig. 36. Pressure oscillation rate of depressurization vs mean chamber pressure, JPL 540 Mod A propellant

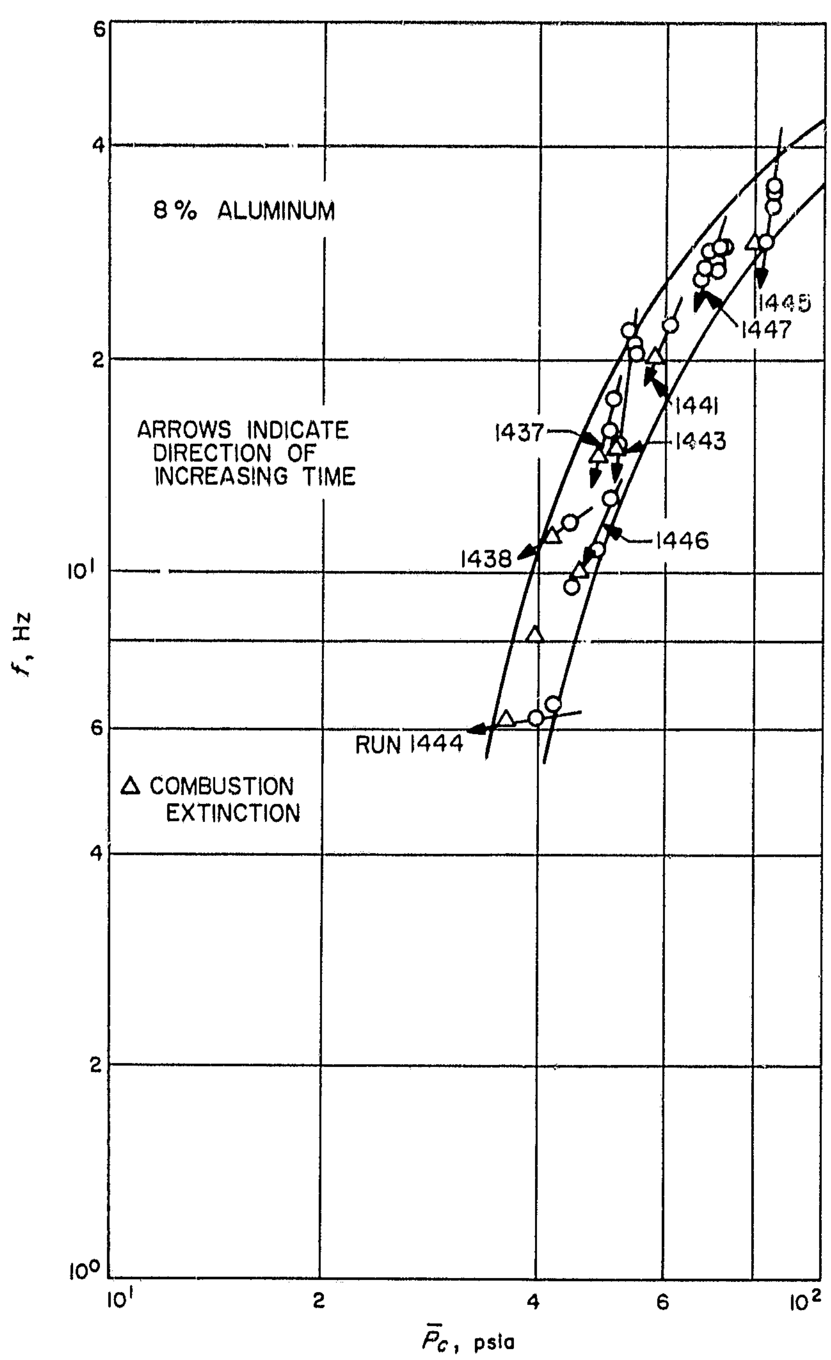

Fig. 37. Pressure oscillation frequency vs mean chamber pressure, JPL 540 Mod B propellant

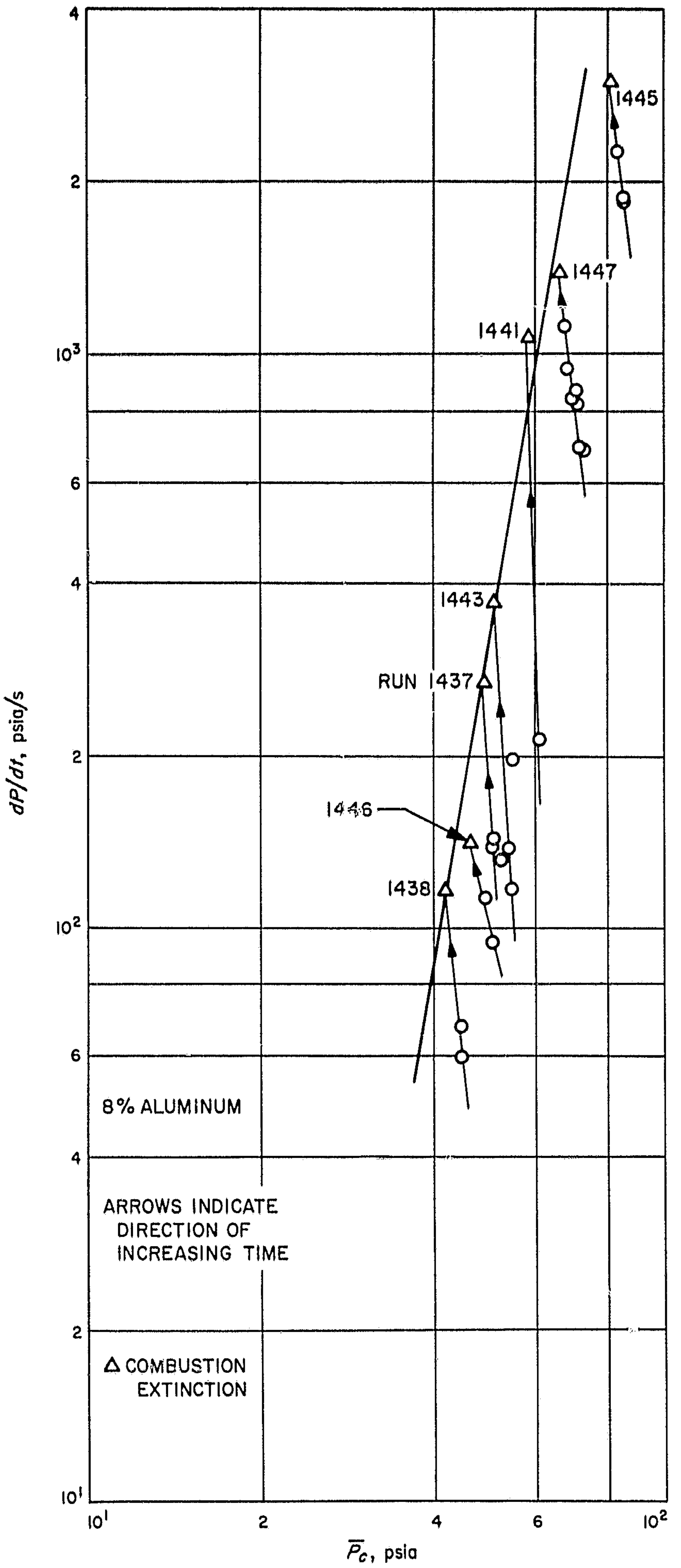

Fig. 38. Pressure oscillation rate of depressurization vs mean chamber pressure, JPL 540 Mod B propellant

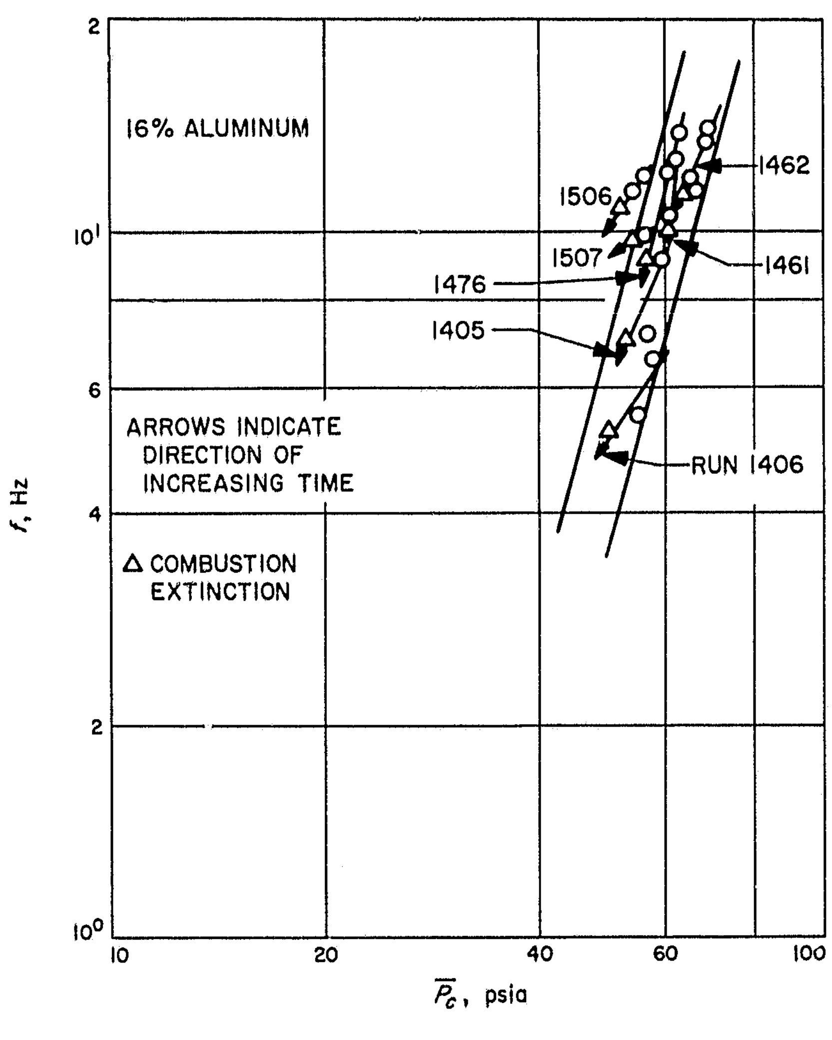

Fig. 39. Pressure oscillation frequency vs mean chamber pressure, JPL 540 propellant

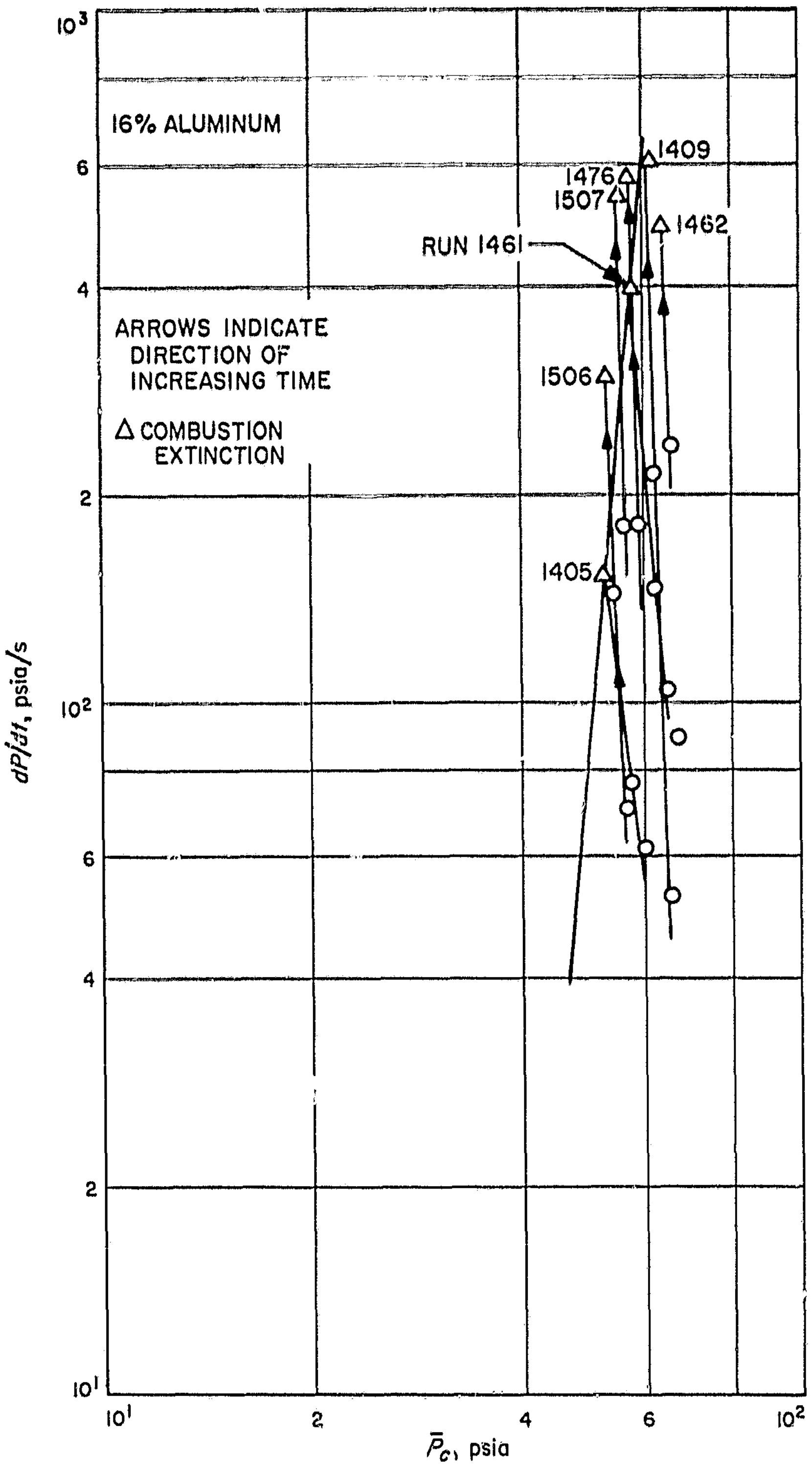

Fig. 40. Pressure oscillation rate of depressurization vs mean chamber pressure, JPL 540 propellant

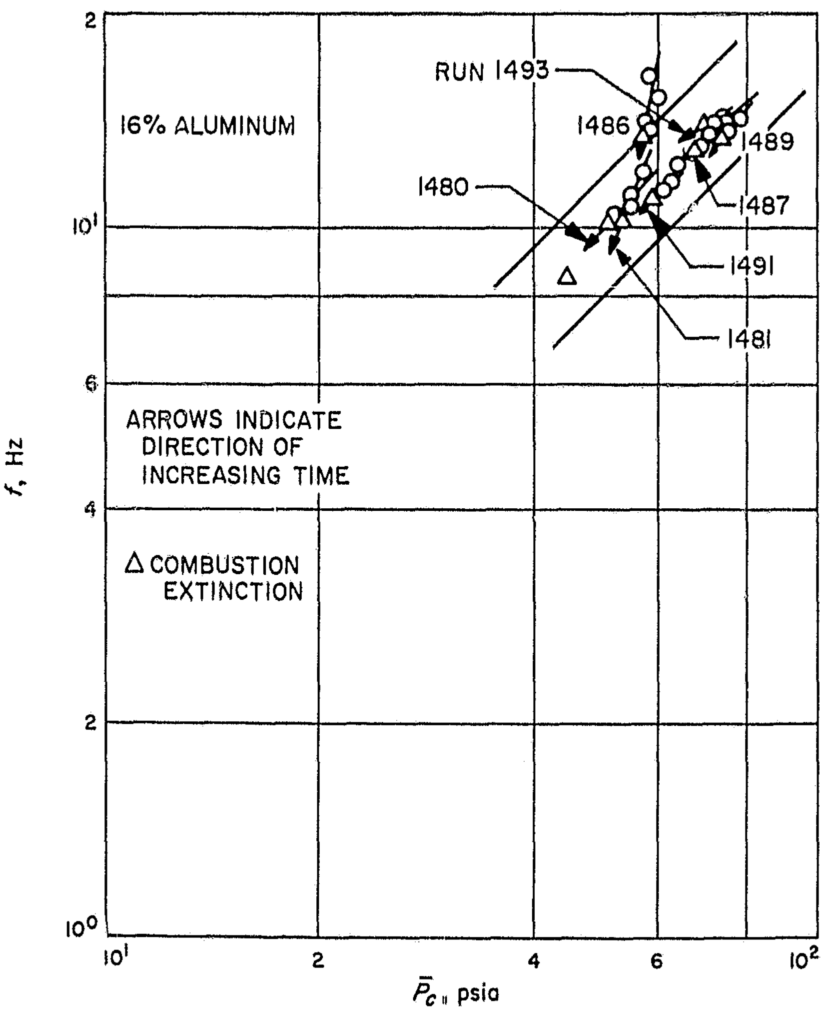

Fig. 41. Pressure oscillation frequency vs mean chamber pressure, JPL 540 Mod 1 propellant

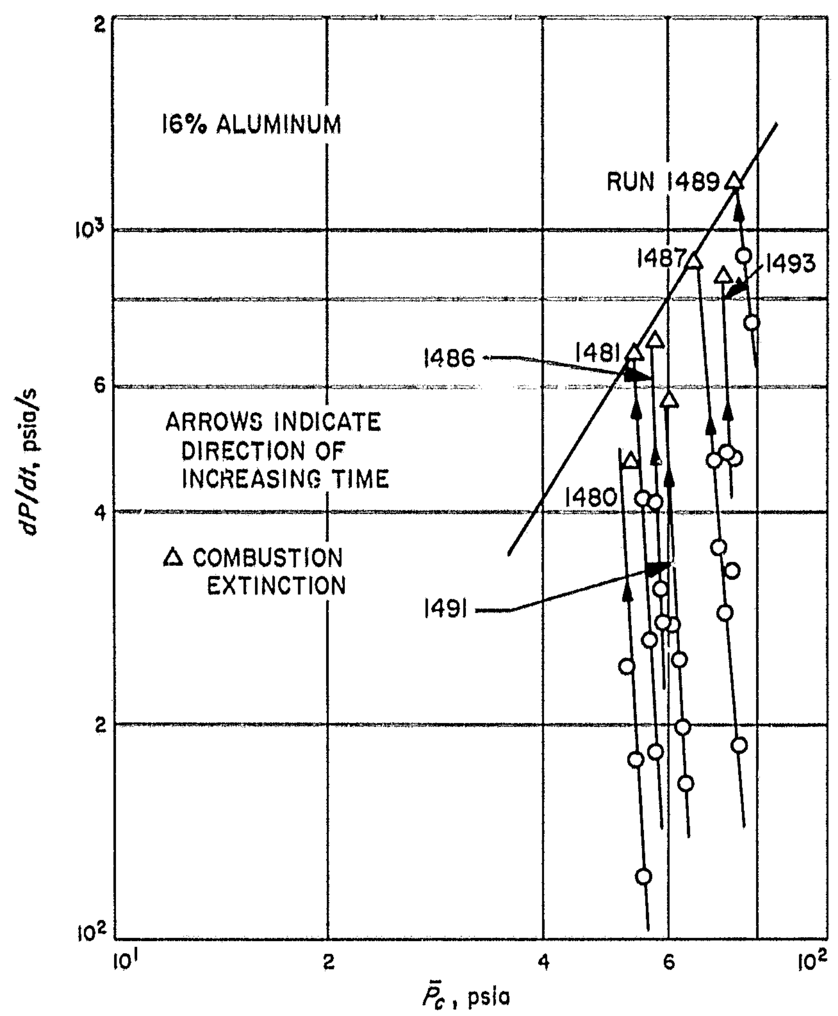

Fig. 42. Pressure oscillation rate of depressurization vs mean chamber pressure, JPL 540 Mod 1 propellant

V. Theoretical Models of Low-Pressure Extinction

Two different philosophies can be followed in attempting to develop theories explaining a certain phenomenon:

(1) Semi-rigorous theories that consider only the variables that are believed of greatest importance, rather than attempting to solve the entire problem completely. The results are used to predict the dependency of the phenomenon on the various factors considered. Such theories can provide (1) qualitative insight into the phenomenon, such as predicting trends, etc.; (2) an approximate basis for experimental data correlation; and (3) qualitative predictions for design applications.

(2) More rigorous theories that hopefully can provide a complete quantitative understanding and explanation of the phenomenon and provide direction and structure for further experimental research. The overall complexity may prohibit obtaining generalized solutions or result in solutions in terms of parameters with unknown values, thereby seriously reducing the utility of the results.

A. Semi-Rigorous Theories

Little theoretical work on the L^* extinction phenomenon itself has been reported to date. Postulating that L^* extinguishment is due to negative pressure perturbations within the rocket chamber, in Refs. 16 and 22 the non-steady solid rocket mass balance expression for dP/dt was substituted into the Paul, et al., von Elbe transient regression rate expressions (Refs. 15 and 23) and, using the mathematical extinction criterion that the instantaneous burning rate drops to zero, the following extinction criterion obtained:

$$L^* \leq \frac{\lambda n \alpha RTC_D}{M a^2 \bar{P}_c^{2n}} \leq \frac{\lambda n \alpha RTC_D}{M \bar{r}_c^2} \qquad (2)$$

where $\lambda = 1$ or 2 depending on whether the Paul, et al. or von Elbe form of the transient regression rate expression is used. The expression is remarkably similar to the previously described low-frequency instability on-set criterion, Eq. (1).[4] In this region of low-pressure instability random pressure perturbations would therefore be of sufficient magnitude to initiate extinction.

The highly-simplified transient combustion models of Paul, et al. and von Elbe make the following assumptions:

(1) Propellant is homogeneous and isotropic

(2) No chemical reaction in the solid phase

(3) Constant propellant surface temperature

(4) Transient state dependency of heat feed-back to the solid on pressure, the same as for steady state

(5) Dependency, during transients, of solid phase thermal profile on pressure, in same manner as during steady state burning

(6) Positive agreement, of thermal gradient in the solid, to the steady state profile for the instantaneous heat flux and rate of regression; i.e., response time of solid thermal gradient short compared to depressurization times.

The model therefore has the fallacy of attempting to describe a transient process with a quasi-steady model.

[4]Expressions are identical if $4(\tau_n)_{cr} = \lambda_n$.

The theory was modified to include thermal lags in the solid thermal gradient (Ref. 24), resulting in the λ term now being an empirical lag correction factor that would theoretically be some function of pressure and the magnitude of the pressure perturbations; this is called the modified Paul theory.

The theory was also extended in Ref. 24 by considering the necessity of avoiding reignition in order that the extinction be permanent. Equation (2) described the conditions necessary for the initiation of extinction. Extinction permanence depended on the avoidance of reignition before the chamber pressure dropped below its minimum ignition pressure, as described by the following expression:

$$\ln (\bar{P}_c/P^*) = (C_D RT/KL^*M) \, [erf^{-1} (P^*/\bar{P}_c)^{1/2}]^2 \qquad (3)$$

where K is an ignition rate constant and P^* is the minimum ignition pressure for the propellant.

A comparison of the theory and experimental data from Ref. 24 is shown in Fig. 43. A curve fit through the data necessitated using unusually large values of the ignition parameters. Figure 44 summarizes much of the published L^* extinguishment data (Ref. 25). Each line corresponds to a different propellant. A portion of the same L^* data plotted in the manner suggested by

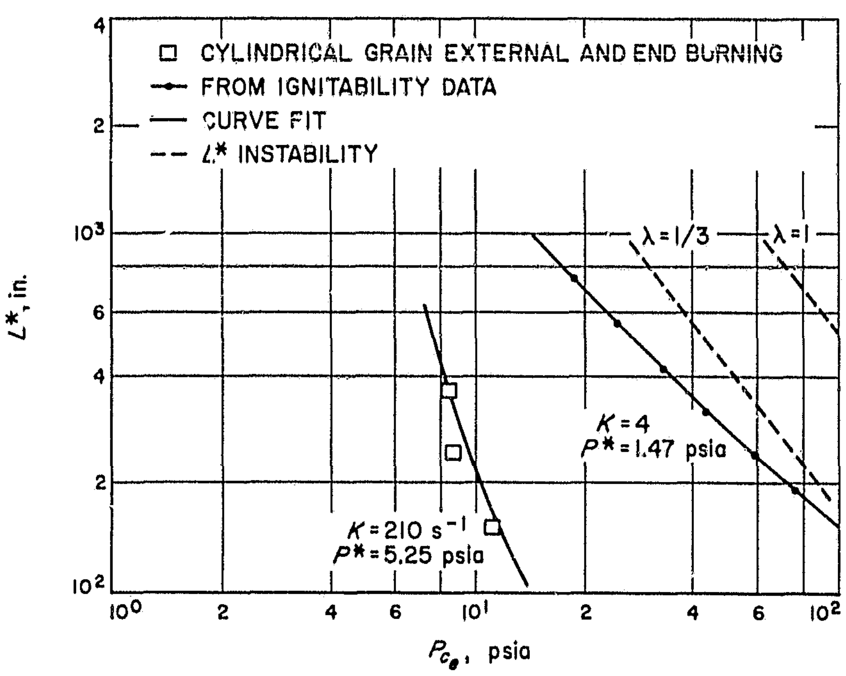

Fig. 43. L^* extinguishment of Aerojet screening test motor (from Ref. 24; used with permission of the United States Air Force Rocket Propulsion Laboratory)

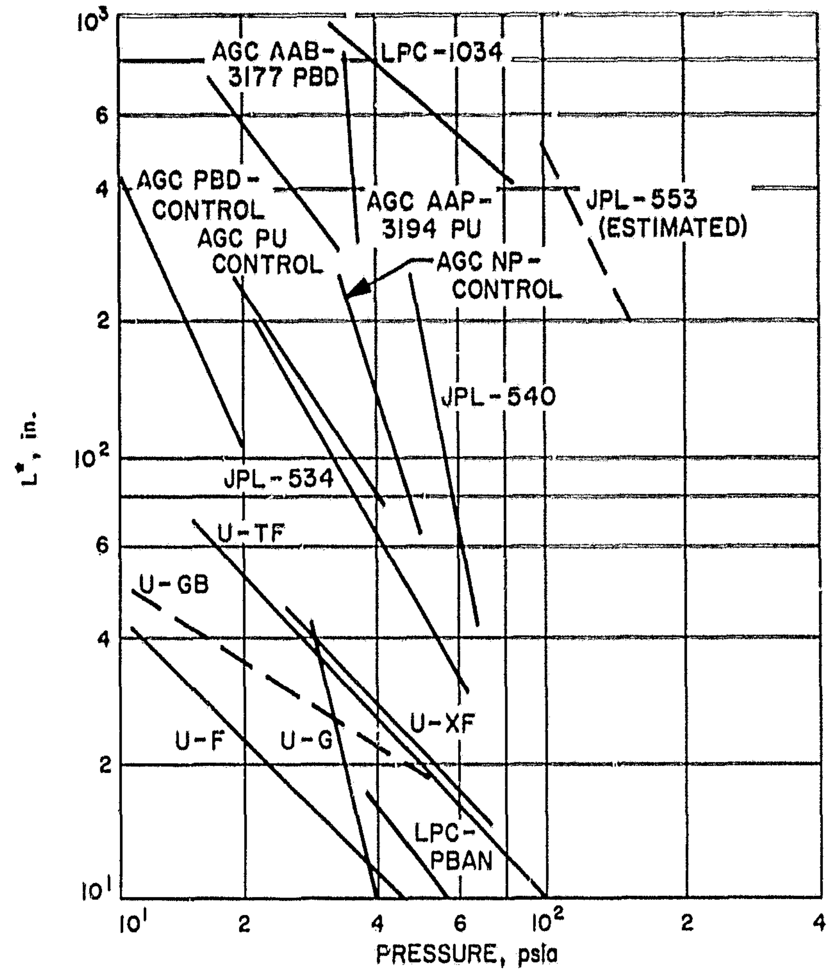

Fig. 44. Summary of L^* extinguishment data (from Ref. 25; used with permission of the author)

the second version of Eq. (2) is shown in Fig. 45 (Ref. 25). The experimental L^*s corresponding to extinction at 50 psia are plotted vs the mean burning rates at 50 psia. The data appear to qualitatively confirm for a variety of propellants the theoretical prediction that the critical L^* varies with the second power of the mean burning rate.

Peterson and co-workers have considered the possibility of L^* extinction being simply the condition of motor mass discharge exceeding mass generated for all motor pressures greater than zero (Fig. 46).[5] The K_n parameter then determines when the motor is in a potentially metastable operating region. The motor L^* is a measure of the fluid capacity and dampening action of the motor, and therefore a measure of the inherent instability in regions of potentially metastable operation. Peterson reported that they had determined this extinction criterion to be fulfilled for a majority of the test data published to date. Variable volume piston motor firings being performed under a current test program

[5]Personal communication with J. A. Peterson, Thiokol Chemical Corporation, Wasatch Division, Brigham City, Utah, Aug. 22, 1967.

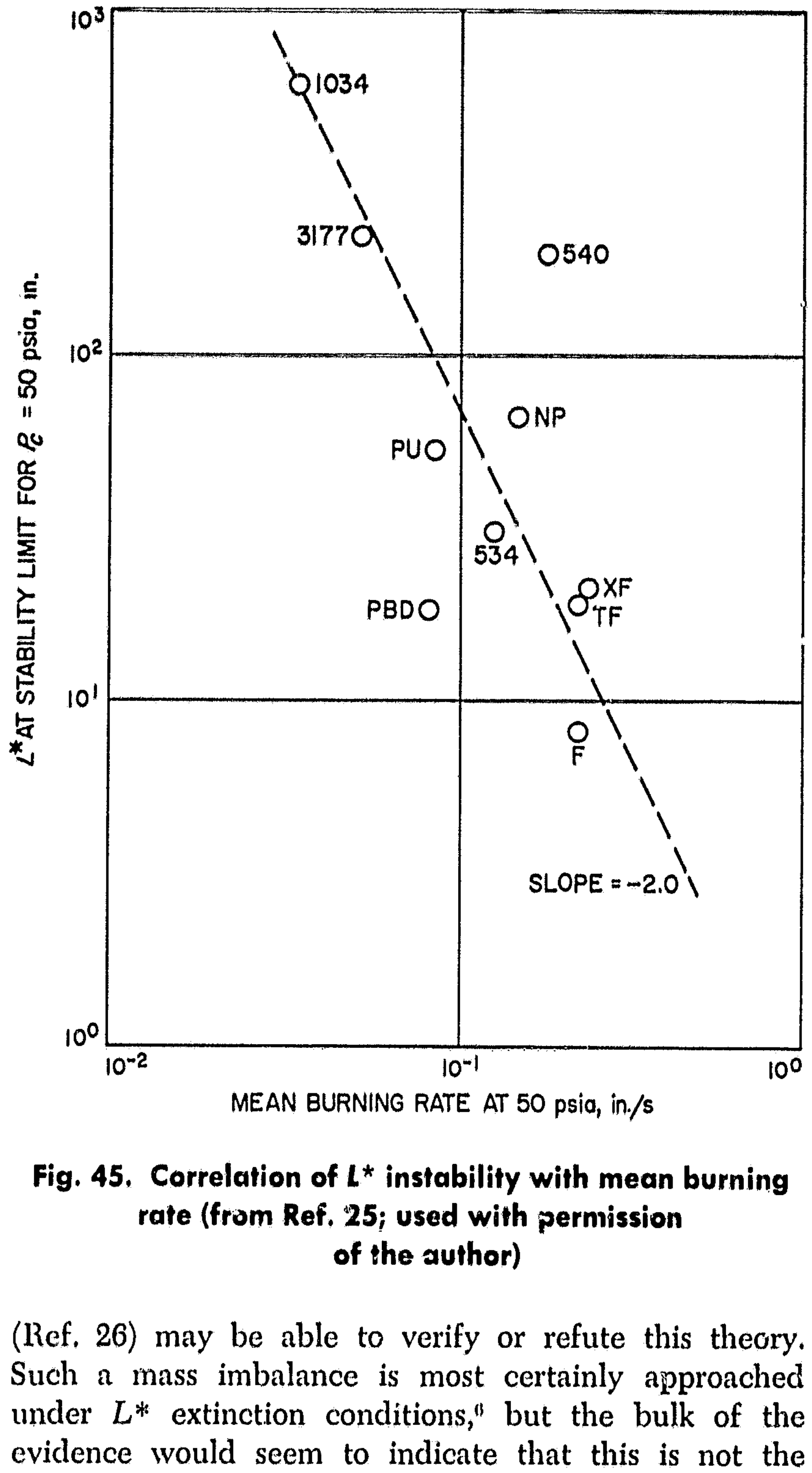

Fig. 45. Correlation of L^* instability with mean burning rate (from Ref. 25; used with permission of the author)

(Ref. 26) may be able to verify or refute this theory. Such a mass imbalance is most certainly approached under L^* extinction conditions,[6] but the bulk of the evidence would seem to indicate that this is not the controlling factor in itself.

The problem of reignition or permanence of extinction appears to be dependent upon very many factors (pressure, gas temperature, erosiveness, chamber configuration, etc.) and to not be amenable to mathematical treatment.

B. Rigorous Theories

Although experimental results are in general agreement with the semi-rigorous theories' prediction that the lower the mean burning rate, the more readily a propellant extinguishes, data presented in this report and elsewhere (Refs. 9 and 27) indicate that the influence of chemical composition and chemical reactions on extinction cannot be completely described by the burning rate alone. A more quantitative explanation of the L^* extinction phenomenon will necessitate an improved understanding of the steady state and transient combustion processes. The present lack of any rigorous theories for L^* extinction is therefore not too surprising. Rather rigorous analyses of combustion quenching by rapid chamber venting (rapid depressurization or dP/dt extinction) are currently being pursued, however (Refs. 9 and 28). The marked similarity in the trends of L^* and dP/dt extinguishment data pointed out by Coates and Cohen (Ref. 25) and the seeming significance of the pressure oscillation rate-of-depressurization on low-pressure L^* extinction reported in Section IV-C point to identical phenomena causing the two types of extinguishment. The current theoretical developments in dP/dt extinguishment should then hopefully be able to be extended to the low-pressure region of self-induced pressure perturbation extinguishment.

[6] The chuffing condition at ignition reported in Ref. 1, for example.

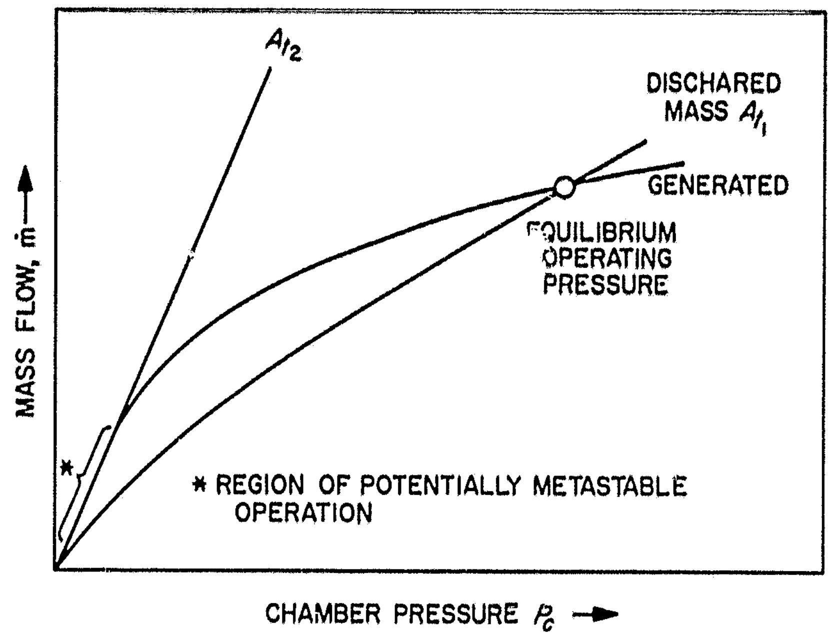

Fig. 46. Motor condition of incipient instability (from material supplied by J. A. Peterson, Thiokol Chemical Corp.)

VI. Summary and Conclusions

The extinguishment data results of a motor firing test program showed the low-pressure instability and extinction to be essentially independent of propellant configuration, a function of the propellant composition, and partially related to the propellant burning rate.

Supplementary tests with a transparent motor gave an indication of the sequence of events occurring in the actual extinction process.

The results of further reduction of the motor firing data provided further information on the point of onset of instability and the frequency dependence of the instability on chamber pressure and L^*, yielded a correlation between the pressure oscillation rate-of-depressurization and mean chamber pressure at extinction, and substantiated the significance of this correlation.

L^* and rapid depressurization extinction are concluded to be due to self-induced and externally induced pressure perturbations respectively and are believed to be two manifestations of the same phenomenon.

Present extinction theories have provided a means of qualitatively correlating extinguishment data for individual propellants using available propellant parameters, but no successful quantitative predictions have been possible. Such predictions will necessitate a greater understanding of the complete solid propellant combustion process.

Nomenclature

- a burning rate coefficient in Vielle's Law
- C_D discharge coefficient
- K ignition rate constant, Eq. (3)
- K_n burning area to nozzle throat-area ratio
- L^* characteristic chamber length (motor free volume/throat-area ratio)
- M molecular weight
- n pressure exponent in Vielle's Law
- P pressure
- P^* minimum ignition pressure
- R universal gas constant
- r propellant burning rate
- T gas temperature
- t time
- α thermal diffusivity
- λ numerical constant or transient correction factor, Eq. (2)
- τ_n chamber time constant, nondimensionalized by $\frac{4\alpha}{\bar{r}^2}$

Superscript

- $-$ steady state

Subscripts

- c chamber
- cr critical
- e extinction

References

1. Anderson, F. A., "Starfinder Motor Development," in *Research Summary* 36-3, Vol. 1, Part 2, pp. 18–20, Jet Propulsion Laboratory, Pasadena, Calif., June 15, 1960.

2. National Defense Research Committee, Office of Scientific Research and Development, *Rocket Fundamentals*, ABL-SR 4, OSRD No. 3992, pp. 67–68, The George Washington University, Washington, D. C., 1944.

3. Anderson, F. A., Strand, L. D., and Strehlow, R. A., *An Experimental Investigation of the Low-Pressure Combustion of Some Solid Propellants* (Title Unclassified), Technical Memorandum 33-134, Jet Propulsion Laboratory, Pasadena, Calif., June 3, 1963 (Confidential).

4. Anderson, F. A., Strehlow, R. A., and Strand, L. D., *Low Pressure Rocket Extinction*, Technical Report 32-509, Jet Propulsion Laboratory, Pasadena, Calif., Nov. 1963. (Also appears in *AIAA J.*, Vol. 1, No. 11, pp. 2669–2671, Nov. 1963.)

5. Akiba, R., and Tanno, M., "Low Frequency Instability in Solid Propellant Rocket Motors," *Proceedings of the First Symposium (International) on Rockets and Astronautics*, Tokyo, 1959.

6. Strand, L. D., "Low-Pressure Combustion Studies," in *Supporting Research and Advanced Development*, Space Programs Summary 37-27, Vol. IV, pp. 49–52, Jet Propulsion Laboratory, Pasadena, Calif., June 30, 1964.

7. Sehgal, R., and Strand, L., "Low-Pressure Combustion of Solid Propellants," *AIAA J.*, Vol. 3, No. 8, pp. 1524–1525, Aug. 1965.

8. Sehgal, R., "Low-Pressure Combustion and Ignition of Solid Rocket Propellants," *Astronaut. Acta,* Vol. 13, No. 2, pp. 167–181, 1967.

9. Jenson, G. E., *A Stop-Start Study of Solid Propellants,* Final Technical Report, Contract NAS 1-6601, NASA CR-66488, UTC 2243-FR, United Technology Center, Sunnyvale, Calif., Nov. 1967.

10. Landsbaum, E., *The Effect of a Shock Wave on a Burning Solid Propellant,* Technical Release 34-97, Jet Propulsion Laboratory, Pasadena, Calif., June 27, 1960.

11. Sehgal, R., and Strand, L., *A Theory of Low-Frequency Combustion Instability in Solid Rocket Motors,* Technical Memorandum 33-130, Jet Propulsion Laboratory, Pasadena, Calif., May 1, 1963. (Also appears in *AIAA J.*, Vol. 2, No. 4, pp. 696–702, April 1964.)

12. Price, E. W., Rice, D. W., and Crump, J. E., *Low-Frequency Combustion Instability of Solid Rocket Propellants, 1 May 1963 to 31 May 1964,* TPR 360, NOTS TP 3524, U. S. Naval Ordnance Test Station, China Lake, Calif., July 1964.

References (contd)

13. West, C. L., and Golding, D. R. V., "Extinguishment Characteristics of Composite Propellants," *Interagency Chemical Rocket Propulsion Group, 3rd Combustion Conference*, CPIA Publication No. 138, Vol. I, pp. 209–212, Silver Spring, Maryland, Feb. 1967.

14. Oberg, C. L., and Huebner, A. L., *Effects of Aluminum on Solid-Propellant Combustion Instability*, Final Report AF49(638)-1575, Rocketdyne Report R-6654, Rocketdyne, a Division of North American Aviation, Inc., Canoga Park, Calif., July 1966.

15. von Elbe, G., "Theory of Solid Propellant Ignition and Response to Pressure Transients" (Article Unclassified). *Bulletin of the 19th Interagency Solid Propulsion Meeting*, CPIA Publication No. 18, Vol. III, pp. 95–127, Silver Spring, Maryland, July 1963 (Confidential).

16. Cohen, N. S., Paul, B. E., and Fong, L. Y., "Solid Propellant Burning Rate Under Transient Heating and Extinguishment via L* Instability," *Bulletin of the 1st ICRPG Combustion Conference*, CPIA Publication No. 68, pp. 491–506, Silver Spring, Maryland, Jan. 1965.

17. Beckstead, M. W., Ryan, N. W., and Baer, A. D., "Nonacoustic Instability of Composite Propellant Combustion," *AIAA J.*, Vol. 4, No. 9, pp. 1622–1628, Sept. 1966.

18. Beckstead, M. W., and Price, E. W., "Nonacoustic Combustor Instability," *Interagency Chemical Rocket Propulsion Group, 3rd Combustion Conference*, CPIA Publication No. 138, Vol. I, pp. 279–289, Silver Spring, Maryland, Feb. 1967.

19. Beckstead, M. W., "Low Frequency Instability: A Comparison of Theory and Experiment," *Western States Section/The Combustion Institute*, Paper 67-13, presented at 1967 Spring Meeting, La Jolla, Calif., April 1967.

20. Coates, R. H., Cohen, N. S., and Harvill, L. R., "An Interpretation of L* Combustion Instability in Terms of Acoustic Instability Theory," *AIAA J.*, Vol. 5, No. 6, pp. 1097–1102, June 1967.

21. Cohen, N. S., "A Theory of Solid Propellant Extinguishment by Pressure Perturbation," *Interagency Chemical Rocket Propulsion Group, 2nd Combustion Conference*, CPIA Publication No. 105, pp. 677–696, Silver Spring, Maryland, May 1966.

22. Strand, L., "Low-Pressure Unstable Combustion Analysis," in *Supporting Research and Advanced Development*, Space Programs Summary 37-26, Vol. IV, pp. 87–93, Jet Propulsion Laboratory, Pasadena, Calif., April 30, 1964.

23. Paul, B. E., Lovine, R. L., and Fong, L. Y., "A Ballistic Explanation of the Ignition Pressure Peak," presented at the *5th AIAA Solid Rocket Conference*, AIAA Preprint 64-121, Palo Alto, Calif., Jan. 1964.

24. Lou, R. L., Landers, L. C., Lovine, R. L., *Theoretical and Experimental Study of Extinguishable Solid Propellants* (Title Unclassified), Final Report AF 04(611)-9962, RPL TR-66-128, Aerojet Report R-0880-82F, Aerojet-General Corporation, Sacramento, Calif., July 1966 (Confidential).

References (contd)

25. Coates, R. L., and Cohen, N. S., "Correlation of Solid Propellant Extinguishment Data," *Interagency Chemical Rocket Propulsion Group, 3rd Combustion Conference*, CPIA Publication 138, Vol. I, pp. 213–218, Silver Spring, Maryland, Feb. 1967.

26. Stepp, E. E., "Combustion Instability Studies of Extinguishable Propellants," paper presented at *Interagency Chemical Rocket Propulsion Group, 4th Combustion Conference*, Menlo Park, Calif., Oct. 1967.

27. Marxman, G. A., and Wooldridge, C. E., *Propellant Combustion Phenomenon During Rapid Depressurization*, Quarterly Report No. 7, Contract NAS 7-389, SRI Project No. PGU-5577, Stanford Research Institute, Menlo Park, Calif., July 26, 1967.

28. Capener, E. L., Dickinson, L. A., and Marxman, G. H., *Propellant Combustion Phenomenon During Rapid Depressurization*, Quarterly Report No. 5, Contract NAS 7-389, SRI Project No. FRU-5577, Stanford Research Institute, Menlo Park, Calif., Feb. 8, 1967.